# Regulatory T Cells in Post-Thrombotic Vessel Repair

**Dissertation**

**zur Erlangung des Grades**

**Doktor der Naturwissenschaften**

**am Fachbereich Biologie**

**der Johannes-Gutenberg-Universität Mainz**


**Fatemeh Zare Shahneh**

**Mainz, November 2018**

Aus der

**Hautklinik und Poliklinik**

Und dem

**Center for Thrombosis and Hemostasis (CTH)**

der Universitätsmedizin Mainz

Dekan:

1. Berichterstatter:

2. Berichterstatter:

Tag der mündlichen Prüfung:

**Statutory Declaration**

"I hereby declare that I have written the submitted dissertation without any unauthorised external support and have only used the sources recognised in the work. All text passages paraphrased or literally from published and unpublished texts, as well as all information from oral sources, are duly indicated and listed according to bibliographical rules. In carrying out my research, I have adhered to the good rules of scientific practice as formulated in the statutes of the Johannes Gutenberg University Mainz."

Mainz, November 2018

Fatemeh Zare Shahneh

**TABLE OF CONTENTS** **Page**

**Page**

**ABSTRACT**

Blood clots form as part of the physiological host response to localised infections and tissue injury, but they cause major disabilities in the context of vascular thrombosis, heart attacks and ischemic stroke. Studies on the role of individual immune cell populations have shown that innate immune cells exclusively trigger thrombus formation while adaptive cells participate in the subsequent inflammation and regulate thrombus resolution. $CD4^+$ $Foxp3^+$ regulatory T (Treg) cells play a pivotal role in the control of autoimmunity and pathological immune responses and also promote non-immunological processes such as tissue homeostasis and tissue repair.

In this work, a specialised population of resident "thrombus-busting" Treg was identified for the first time. These specialist cells develop in venous thrombus, are activated by cytokines from monocytes and regulate thrombus resolution by imposing phenotypic and functional changes in the myeloid compartment.

Understanding the Treg population in venous thrombi may provide novel therapeutic strategies that can improve recovery in thrombosis patients and facilitate the restoration of organ function in chronic thrombo-inflammatory diseases.

**Zusammenfassung**

Blutgerinnsel bilden sich als Teil der physiologischen Wirtsreaktion auf lokalisierte Infektionen und Gewebeschäden, verursachen aber im Rahmen von Gefäßthrombosen, Herzinfarkten und ischämischen Schlaganfällen schwere Behinderungen. Studien zur Rolle einzelner Immunzellpopulationen haben gezeigt, dass die Blutgerinnung exklusiv durch angeborene Immunzellen ausgelöst wird, adaptive Immunzellen jedoch an der anschließenden Entzündung beteiligt sind und die Gerinnselsauflösung regulieren. $CD4^+$ $Foxp3^+$ regulatorische T (Treg)-Zellen spielen eine zentrale Rolle bei der Unterdrückung von Autoimmunität und der Begrenzung pathologischer Immunantworten, fördern aber auch nicht-immunologische Prozesse wie Gewebehomöostase und Gewebereparatur.

In dieser Arbeit wurde erstmals eine spezialisierte Population residenter "Gerinnsel-auflösender" Treg identifiziert, die sich in venösen Blutgerinnseln entwickelt, durch Zytokine aus Monozyten aktiviert wird und die Thrombenauflösung durch phänotypische und funktionelle Veränderungen im myeloiden Kompartiment reguliert.

Das Verständnis der Rolle von Treg bei der Gerinnselauflösung kann Ansatzpunkte für neue therapeutische Strategien bieten, die die Genesung bei Thrombosepatienten und die Wiederherstellung der Organfunktion bei chronischen thrombotisch-entzündlichen Erkrankungen verbessern.

# 1. INTRODUCTION

## 1.1. Venous Thromboembolism

Venous thromboembolism (VTE), which includes deep vein thrombosis (DVT) and pulmonary embolism (PE), is a common cause of morbidity and mortality worldwide. Blood clots, termed thrombi, often form in the deep veins such as those of the leg, arm, pelvis, abdomen, or around the brain. PE is a potentially life-threatening complication of DVT that emerges when blood clots detach and travel through the blood stream to the pulmonary arteries (Di Nisio et al., 2016). If clots do not completely resolve, DVT patients develop a chronic post-thrombotic syndrome (PTS) and chronic thromboembolic pulmonary hypertension (CTEPH) leading to heart failure (Bochenek et al., 2017).

VTE poses a major public health threat as the third most common cardiovascular disease after acute coronary syndrome and stroke. The expected average annual frequency of VTE among individuals of European ancestry ranges from 104 to 183 cases per 100,000 people per year, with a quarter of cases resulting in death. Approximately 30% of patients develop recurrence within the next six months to ten years with higher rates of recurrence in older patients (Heit et al., 2016; & Henke et al., 2011). VTE is currently managed with a combination of anticoagulants such as heparin, low molecular weight heparin, warfarin, fondaparinux and direct oral anticoagulants (DOACs). Severe cases require further measures, such as thrombolytic therapy or embolectomy (Streiff et al., 2016). The goal of VTE treatment is to prevent an existing clot from propagation, and the main concern with anticoagulant therapy is bleeding (Evans et al., 2014). The critical limitation of these medications is that they do not dissolve the existing thrombi in the acute phase of VTE, and the possibility of long-term complications due to residual clot is a matter of debate (De Caterina et al., 2016). Therefore, DVT would benefit from therapies that accelerate thrombus resolution.

### 1.1.1. Mouse Models of Venous Thrombosis

DVT mouse models allow us to investigate the underlying biology of the disease.

They are important despite differences between mice and human in life expectancy, body size, vessel size and genetics because thrombotic human veins are not operated on and therefore inaccessible (Diaz et al., 2010). In the inferior vena cava (IVC) stenosis model thrombogenesis is initiated by 80-90% blood flow reduction which reproduces a frequent trigger and resembles the time course (kinetics), histological features, and clinical presentation of acute and chronic DVT in humans (Diaz et al., 2012). In this mouse model, venous thrombosis is induced without endothelial damage or surgical trauma. Venous blood clot formation can be separated into several phases. Acute DVT is defined as the presence of a thrombus for up to 2-3 days (Figure 1.1), while subacute and chronic DVT defines a thrombus that has been present for 7-21 days (Geddings et al., 2014; & Schönfelder et al., 2017).

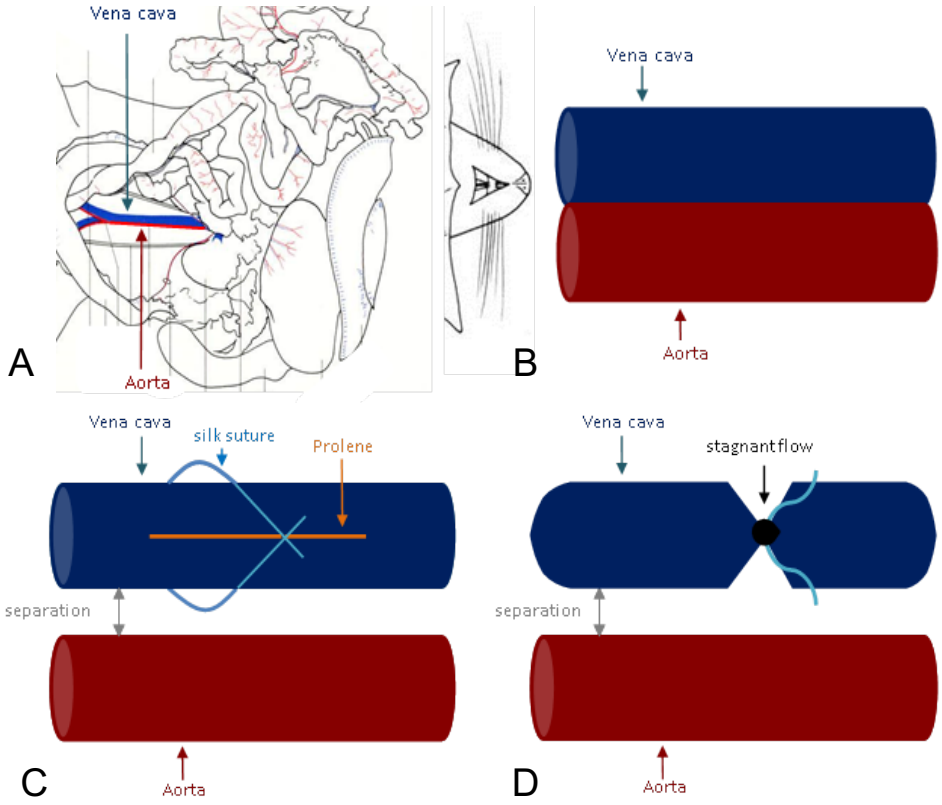


**Figure 1.1. IVC stenosis process.** A) Organ area. (B, C, D) Schematic representation of the aorta and the vena cava and the production of the IVC ligature, which induces thrombosis by stagnating blood flow.

### 1.1.2. The Formation of Venous Thrombi

Massive leukocyte accumulation precedes the development of DVT in response to restriction of venous blood flow. Healthy endothelial cells maintain vessel hemostasis through the modulation of procoagulants and anticoagulants, vasoconstrictors and vasodilators, and cell adhesion molecules and inflammatory cytokines. However, once the endothelium becomes activated, such as in response to decreased blood flow, endothelial cells adopt a pro-inflammatory phenotype that leads to subsequent adherence of immune cells, particularly platelets, circulating neutrophils and monocytes (Furie et al., 2008; & Mackman., 2012). In the IVC ligation model leukocytes start to adhere and roll on the venous endothelium within only one hour of depressed venous blood flow (Roumen-Klappe et al., 2009), whereas they barely interacted with the endothelium when blood flow is unperturbed, such as in sham-operated animals. Leukocyte accumulation increases over time, and after 5-6 hours leukocytes cover the entire endothelial surface (Esmon et al., 2008).

Neutrophils may initiate venous thrombosis through the release of neutrophil extracellular traps (NETs). NETs comprise a matrix of DNA and histones which are released in a process termed NETosis. NETs can bind to platelets via von Willebrand factor (vWF) and activate them in the setting of venous thrombosis propagation in mice. The polyanionic NET surface, when in contact with platelets, also activates intravascular tissue factor (TF) and coagulation factor XII (FXII) to promote both the extrinsic and intrinsic pathway of coagulation. Neutrophil-driven coagulation leads to DVT stabilisation in the setting of reduced venous blood flow (Saha et al., 2011; & Mackman., 2008).

Platelets are activated and recruited to the damaged site during the acute phase of DVT, where they bind to sub-endothelial matrix proteins (collagens and vWF) via cell-surface receptors such as the vWf receptor GPIba. In parallel with the platelet activation and aggregation at the site of vessel damage, the coagulation cascade enhances a stable thrombus. TF expressed by endothelial cells, platelets, and monocytes initiates a tightly regulated extrinsic coagulation pathway. The interaction of monocyte-derived TF with factor VIIa triggers factor X activation, thrombin formation and finally the conversion of fibrinogen into fibrin (Esmon., 2009; Schulz et al., 2013; & Engelmann et al., 2013). Platelets also stimulate the up-regulation of TF

expression in monocytes. However, the mechanisms that lead fibrin formation remain unclear. A shift towards neutrophils and monocytes appears by days 2-4 in the subacute phase of DVT and they become the predominant inflammatory cells in both the vein wall and the thrombus (Swystun et al., 2016; & Von Brühl et al., 2012). Moreover monocyte depletion is highly associated with a reduction in thrombus size, thrombus area, and thrombus weight during the acute phase.

### 1.1.3. Thrombus Propagation

Coagulation and inflammation are intricately linked processes. Following blood clotting, a sequence of pro-inflammatory mechanisms promotes thrombus propagation and adjacent vein wall inflammation. Waves of leukocytes invade the vessel wall (and thrombus), starting with neutrophils and followed by inflammatory monocytes (Esmon et al., 2008).

Inflammatory biomarkers of DVT include elevated levels of IL-6, IL-8, P-selectin, CCL2, CXCL1, CXCL5, MCP-1 and CRP (Roumen-Klappe et al., 2009). The chemotactic stimuli produced by the thrombus such as IL-8 and MCP-1 play an important role in the recruitment of monocytes to the injured vessel (Shi et al., 2011). It has recently been shown that growth arrest-specific 6 (Gas6) promotes inflammatory monocyte ($Ly6C^{hi}$ $CCR2^{hi}$ $CX3CR^{lo}$) migration in thrombosis that is possibly mediated via c-Jun N-terminal kinase (JNK) (Ley et al., 2011).

### 1.1.4. Thrombus Resolution and Vein Wall Healing

Thrombus resolution and vein wall remodelling are influenced by inflammatory events that accompany myofibroblast activation/accumulation and angiogenesis, followed by collagen deposition to return to tissue homeostasis. However, dysregulation of any cells or stage of thrombus healing could lead to fibrosis and the accumulation of extracellular matrix (ECM) (Laurance et al., 2017). Following an early, transient recruitment of neutrophils, myeloid mononuclear cells infiltrate the injured vein and thrombus. After DVT induction, large numbers of inflammatory monocytes are

recruited as an important source of chemokines, matrix metalloproteinases (MMPs) and other inflammatory mediators (Wakefield et al., 2008). After the early inflammatory phase diminishes, and in the reparative phase of DVT, the myeloid cells shift from a pro-inflammatory ($Ly6C^{hi}$ $CCR2^{hi}$ $CX3CR^{lo}$) to a wound-healing or reparatory ($Ly6C^{lo}$ $CCR2^{lo}$ $CX3CR^{hi}$) phenotype, a timely conversion that is critical for appropriate thrombus resolution and tissue healing (Figure 1.2) (Henke et al., 2009). Reparatory monocyte recruitment increases the production of proteases such as plasmin and MMPs in order to remove excess ECM during the resolution phase. This mirrors the process that occurs in the first few days of the inflammatory phase, where MMPs are secreted by inflammatory monocytes to repair the injured tissue from damaged ECM (Nahrendorf et al., 2010). Furthermore, reparatory monocyte recruitment inhibits apoptosis and promotes mesenchymal cell proliferation. MMPs are a cluster of highly conserved, highly regulated enzymes that degrade an array of ECM proteins and mediate the remodelling of the ECM in acute and chronic fibrotic diseases (Hendrix et al., 2017; & Deatrick et al., 2017). Recent studies on thrombus resolution have shown an increase in collagen I and III gene expression, as well as an increase in MMP-2, 8, 9, and 13 gene expression and activity (Beaudeux et al., 2004; & Deatrick et al., 2013).

The fibrinolytic system also controls DVT induced by inflammation and play a key role in thrombus resolution. Plasmin lyses a thrombus by degrading fibrin. Both monocytes and neutrophils can regulate the activity of the fibrinolytic pathway. They also express plasminogen receptors such as enolase and Annexin II, which localise plasminogen to the leukocyte surface (Nguyen et al., 2013). This enhances plasminogen activation by tissue-type plasminogen activator (t-PA) and urokinase-type plasminogen activator (u-PA) and mediates cell migration and tissue remodelling. In venous thrombus resolution, monocyte-associated u-PA activity is the most important plasminogen activator (Henke et al., 2007).

ECM remodelling events that accompany collagen deposition and MMP expression and activation are only present during the later phases at both the vein wall and the thrombus. In venous thrombosis, endothelial progenitor cells are recruited during the repair phase, and contribute to neovascularisation and tissue damage contraction. These pluripotent cells with features of vascular smooth muscle cells (VSMC),

fibroblasts, and endothelial cells play a critical role in the vascular injury healing response (Baldwin et al., 2012; & Nissinen et al., 2014). The VSMC might directly mediate the fibroproliferative response, and cause further monocyte influx. Fibrocytes also convert into myofibroblasts expressing α-smooth muscle cell (α-SMA) and secreting more ECM components which benefits thrombus resolution (Hinz et al., 2001; & Caley et al., 2015). Furthermore, the vascular fibrotic stage may occur due to direct endothelial-to-mesenchymal transformation (EndMT). This process is characterised by an increase in mesenchymal antigens, such as α-smooth muscle cell (α-SMA) and fibronectin (FN), and a decrease in endothelial antigens such as vascular endothelial (VE) cadherin and CD31 in endothelial cells (Zeisberg et al., 2007; & Kellermair et al., 2013).

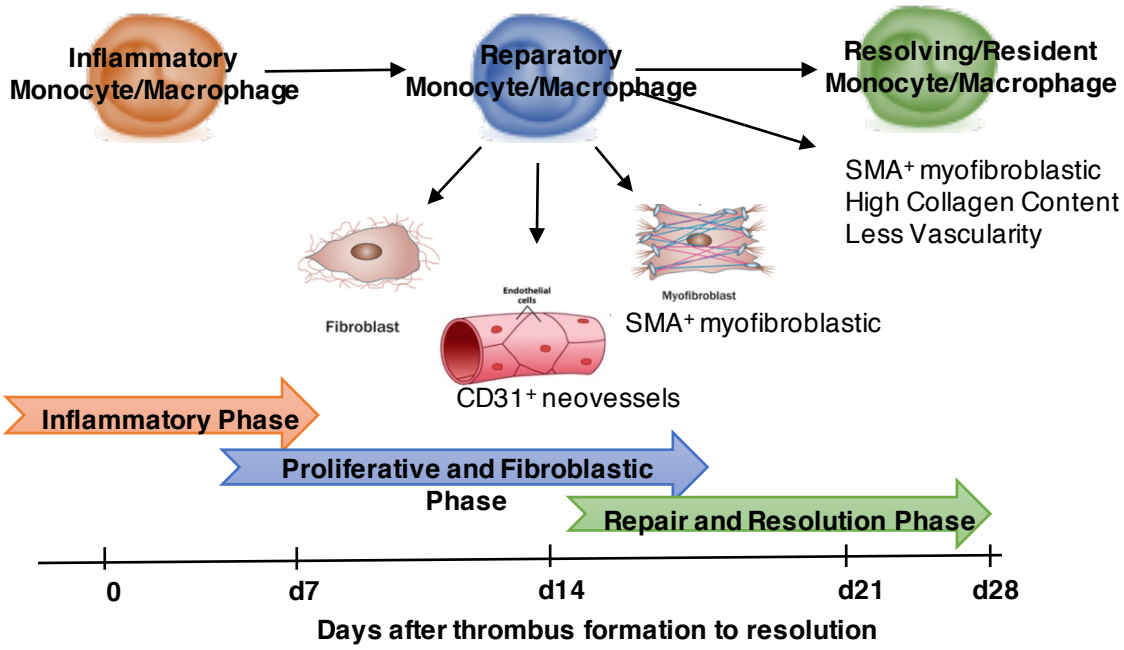


**Figure 1.2. Overlapping phases of thrombus repair and resolution in the context of myeloid cells.** In the early stages of thrombus formation (clotting), inflammatory monocytes infiltrate the site of tissue activation, and then undergo phenotypic and functional changes to become reparatory in the proliferative phase and leading to myofibroblast activation and neovascularisation in the resolution phase. The healing process regulated by reparatory and resident monocytes/macrophages results in effective thrombus resolution and tissue remodelling.

### 1.2. Regulatory T cells

Regulatory T (Treg) cells are a specialised subset of $CD4^+$ T cells that modulate the activities of a wide variety of immune cells to preserve immune homeostasis. Treg cells are characterised by the stable expression of the lineage-specific transcription factor Foxp3, an X chromosome-encoded member of the forkhead transcription factor family, and constitutive high expression of the interleukin 2 (IL-2) receptor α-chain CD25 (Fontenot et al., 2003; & Ding et al., 2012).

Analysis of $Foxp3^{DTR}$ knock-in and Foxp3-DTR BAC transgenic mice revealed that the expression of Foxp3 in T cells is essential for the differentiation of Treg cells and acquisition of suppressive function. Accordingly, loss-of-function mutations in the Foxp3 gene cause fatal and spontaneous early-onset autoimmunity in mice ('scurfy' mouse) and human immunodysregulation polyendocrinopathy enteropathy X-linked (IPEX) syndrome (Sakaguchi et al., 2008).

Apart from their constitutive Foxp3 and CD25 expression, Treg cells exhibit several phenotypic and molecular characteristics, including an inability to proliferate and produce IL-2 in response to T cell receptor (TCR) stimulation in vitro, expression of low amounts of IL-7Rα chain (CD127), and higher amounts of cytotoxic T lymphocyte antigen 4 (CTLA-4), tumour necrosis factor receptor superfamily member 18 (TNFRSF18 known as GITR) and inducible T cell co-stimulator (ICOS) (Li et al., 2015; & Fu et al., 2014).

#### 1.2.1. Treg Origin

The majority of Treg cells develop in the thymus. The differentiation of $Foxp3^+$ thymocytes depends on high-affinity TCR interaction with self-peptide/MHC class II complexes expressed by thymic stromal cells, IL-2 receptor signalling, accessory molecules (CD28) and their ligands (CD80 and CD86) (Figure 1.3) (Sakaguchi et al., 2008). Beside TCR stimulation, various experimental conditions favour induction of Foxp3, including constitutive NF-κB signalling, loss of maintenance DNA methyltransferase activity, deficiency in mTOR or sphingosine-1 phosphate receptor type 1 (S1P1), and reduction of PI3K signalling (Levine et al., 2014).

Other essential signals for Treg cell differentiation include IL-2, IL-7 and IL-15, which act through the common gamma-chain (γc) cytokine receptors. IL-2 or IL-2Rα chain

deficiency decreases Foxp3⁺ thymocyte numbers by around 50%, whereas loss of IL-15 or IL-7 alone does not prevent Treg cell development. Nonetheless, γc cytokine receptor–deficient mice with a combined ablation of IL-2, IL-7, and IL-15 completely lack Foxp3⁺ thymocytes and peripheral Foxp3⁺ T cells. (Cheng et al., 2013; & Malek et al., 2010).

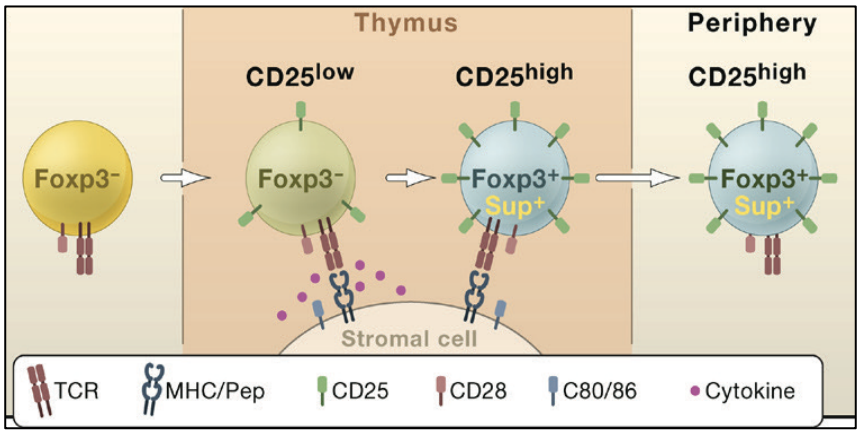


**Figure 1.3. Thymic development of Foxp3⁺ cells.** Development of Foxp3⁺ Treg cells in the thymus involves interaction with thymic stromal cells via different molecules.

### 1.2.2. Treg Trafficking

After leaving the thymus, a small population of tTreg cells settle as naïve Treg cells in the secondary lymphoid organs such as the spleen and lymph nodes. Upon migration into lymphoid organ, Tregs express a variety of homing receptors, including adhesion molecules and chemokine receptors. In the peripheral lymph nodes, most Tregs express CCR7, CCR4, CCR6, CXCR4, and CXCR5 at high levels (Huang et al., 2016).

Around 30% of Treg cells express CD103 (integrin αEβ7) and a large portion (~50%) highly express CD62L (L-selection), which interacts with the vascular addressins such as CD34 expressed by the endothelium in lymph nodes. The expression of these homing receptors in Treg controls their trafficking and localisation during immune responses (Wei et al., 2006; & Li-Fan et al., 2009).

### 1.2.3. Peripheral Generation of Treg Cells from Naive T Cells

In addition to their thymic development (tTreg), Treg cells can also evolve from peripheral naive $CD4^+$ T cells under particular conditions in various tissues (pTreg). Specifically, in vitro antigenic activation of naive $CD4^+$ T cells in the presence of the TGF-β and in the absence of inflammatory cytokines, results in pTreg cell development. Conversely, Foxp3 expression by tTregs is TGF-β independent, as evidenced by normal tTreg cell frequency and function in TGF-β-deficient mice. (Horwitz et al., 2008; & Fahlén et al., 2015). Moreover, IL-10 and retinoic acid assist the naive T cells differentiation to pTreg; this occurs especially in response to orally administered protein antigens. High amounts of IL-2 are also required for the TGF-β-mediated induction of Foxp3 in peripheral $CD4^+$ T cells in vitro and prevents their differentiation into T helper 17 cells (Dhamne et al., 2013).

Unfortunately, there is not yet a marker that is reliably able to distinguish between pTreg and tTreg cells. Markers suggested to distinguish tTregs, for example the transcription factor Helios and Neuropilin-1 turned out to be inducible in pTreg cells under certain conditions (Kim et al., 2015). In-depth analysis of the Foxp3 locus, however, revealed differential CpG DNA methylation patterns (differentially methylated regions [DMRs]) of the Foxp3 Treg specific demethylation region (TSDR) in the two Treg subsets (Gottschalk et al., 2012).

### 1.2.4. Treg-Mediated Suppression

Numerous different mechanisms of Treg-mediated suppression have been suggested, in both lymphoid and non-lymphoid tissues in several experimental settings. The choice of mechanism seems to be influenced by the tissue site, target cell and characteristics of the inflammatory response (Sojka et al., 2008).

It has been suggested that suppressive mechanisms include the production of immunosuppressive cytokines such as IL-10, IL-35 and TGF-β and the metabolic inhibition of effector cells through adenosine or cyclic AMP (Liston et al., 2014). High-level IL-2R (CD25) expression on Treg cells is suggested to deprive effector T cells of

IL-2 and inhibit their proliferation. Activated Treg-expressed CTLA-4 can down-regulate the co-stimulatory ligands CD80 and CD86 on antigen presenting cells or stimulate dendritic cells (DCs) to form the enzyme indoleamine 2, 3-dioxygenase (IDO), which catabolises the essential amino acid tryptophan to kynurenines that are toxic to T cells (Shevach., 2009). Similarly, T cell Ig and ITIM (TIGIT) on Tregs appears to induce the production of immunosuppressive cytokines IL-10 and TGF-β by DCs (Kurtulus et al., 2015).

### 1.2.5. Functional Specialisation of Regulatory T Cells

In addition to differences based on their location, Tregs can be classified into functional subsets including a central population, distinctive effector Treg populations, memory Treg populations, and polarised tissue-resident Treg populations. Activated effector Treg in the blood and secondary lymphoid organs comprise a minor population. Tissue-resident Treg cells reside long-term in non-lymphoid tissues for local immune regulation. Recent studies reveal an importance of several individual chemoattractant and homing receptors in Treg cell recruitment to non-lymphoid tissue especially during inflammation for appropriate tissue function (Feng et al., 2015).

### 1.2.6. Treg Localisation in Distinct Immune Responses

Thymus-derived Tregs are a largely homogenous population of $CD4^{+}$ $CD25^{hi}$ $FoxP3^{hi}$ cells that preferentially express the lymph node homing receptor L-selectin (CD62L) and reside in secondary lymphoid tissues. After entering the periphery, some Treg cells rapidly become activated and gain phenotypic characteristics of effector or memory T cells. Many become $CD44^{hi}$ and up-regulate homing receptors such as CCR5, CCR6, CXCR3 CXCR4, and CXCR5, which allow them to access non-lymphoid sites and display distinct homeostatic behaviours (Table 1.1) (Safinia et al., 2015; & Rosenblum et al., 2016).

| Regulatory T cells | | | | | |
|---|---|---|---|---|---|
| | **Resting** | **Activated effector** | **Central memory** | **Effector memory** | **Tissue-resident** |
| **Selected phenotypic markers** | $CD25^{hi}$<br>$CD44^{lo}$<br>$CD69^{lo}$<br>L-$selectin^{hi}$<br>$CD127^{lo}$<br>$KLRG1^{lo}$<br>$CTLA4^{lo}$ | $CD25^{lo/-}$<br>$CD44^{hi}$<br>$CD69^{hi}$<br>L-$selectin^{lo}$<br>$CD127^{lo}$<br>$KLRG1^{hi}$<br>$CTLA4^{hi}$ | $CD25^{hi}$<br>$CD44^{hi}$<br>$CD69^{hi}$<br>L-$selectin^{hi}$<br>$CD127^{hi}$<br>$KLRG1^{lo}$<br>$CTLA4^{hi}$ | $CD25^{hi}$<br>$CD44^{hi}$<br>$CD69^{hi}$<br>L-$selectin^{lo}$<br>$CD127^{hi}$<br>$KLRG1^{hi}$<br>$CTLA4^{hi}$ | $CD25^{hi}$<br>$CD44^{hi}$<br>$CD69^{hi}$<br>L-$selectin^{lo}$<br>$CD127^{hi}$<br>$KLRG1^{lo}$<br>$CTLA4^{hi}$ |
| **Chemokine receptors** | $CCR7^{hi}$ | $CCR7^{lo}$ | | | |
| **Transcription factors** | $FOXP3^{hi}$ | $FOXP3^{hi}$ | $FOXP3^{hi}$ | $FOXP3^{hi}$ | $FOXP3^{hi}$ |

**Table 1.1. Selected markers for resting, effector, memory, and tissue-resident regulatory T cell subsets.**

Both antigens and inflammatory stimuli such as cytokines can further drive Treg cell differentiation. Recent evidence has shown how effector and tissue-resident Tregs can polarise and alter their transcriptional programs with distinct suppressor mechanisms to adapt to tissues or the inflammatory context (Rosenblum et al., 2016). T helper 1 (Th1) cell–type Treg, a $CXCR3^{+}$ Treg subtype, was described as being dependent on the T-bet transcription factor for differentiation and function under Th1 cell inflammatory conditions (Toomer et al., 2016). By contrast, T helper 2 (Th2) cell–type Tregs depend on transcription factors IRF4 and GATA3, otherwise required for differentiation of Th2 effector cells, to suppress the Th2-type

inflammatory responses. During Th17 cell-mediated immune responses, Th17 cell-type Tregs differentiate at sites of inflammation under the influence of STAT3 and CCR6. Hence, selective ablation of STAT3 in Treg cells leads to uncontrolled Th17-dependent pathology (Tan et al., 2016; & Tanoue et al., 2016).

Finally, another important subtype is follicular Tregs which express the transcriptional repressors Blimp-1, Bcl-6, ICOS and SAP and the chemokine receptor CXCR5 and regulate B cell responses in germinal centres (Figure 1.4) (Campbell et al., 2011). Indeed, transcription factors necessary in distinctive T helper cell lineages appear to also play a similar and central role in Treg cell homeostasis and function in individual tissue and inflammatory settings.

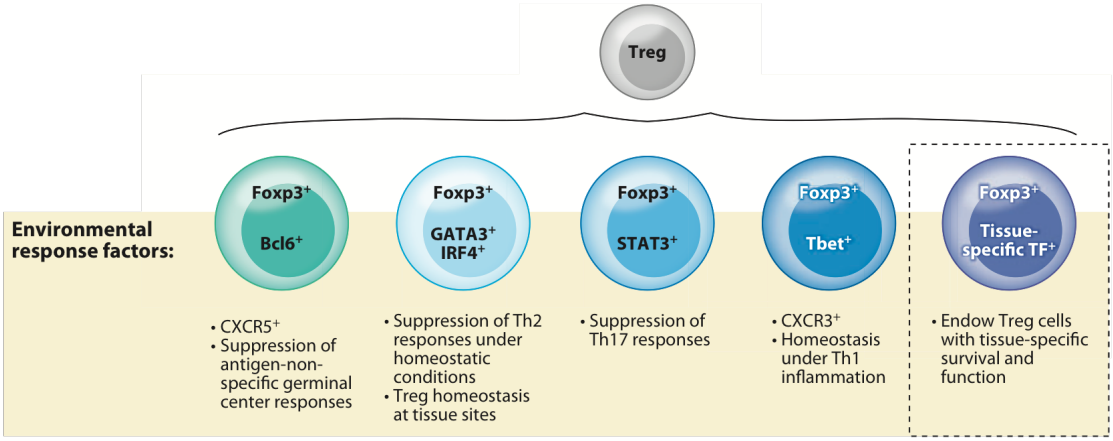


**Figure 1.4. Regulatory T cells become specialised through the activation of transcription factors in response to different stimuli.** Upon instruction by the tissue environment, Treg cells polarise and gain the expression of specific transcription factors in cooperation with Foxp3.

### 1.2.7. Regulatory T cell in Inflamed non-lymphoid Tissues

Treg cells can be present in healthy tissues in small numbers even in the absence of overt inflammation. Inflammation, however, seems to attract Tregs and their recruitment appears to have a decisive influence on the course of disease (Sage et al., 2016, Burzyn et al., 2013). Treg populations that regulate non-lymphatic tissues differ from those in lymphatic organs in terms of their antigen specificity as well as the molecules and regulated cells that result (Josefowicz et al., 2009). Particular examples are Tregs in visceral fat tissue (VAT) (Panduro et al., 2016; & Feuerer et al., 2009) and Tregs that accumulate in injured muscle (Figure 1.5). While VAT Tregs

mainly interact with myeloid cells, muscle Tregs also produce molecules that act directly on muscle cells and stimulate their regeneration (Cipolletta et al., 2012; Burzyn et al., 2013; & Arpaia et al., 2013). Further populations of specialised Treg cells were observed in ischemic stroke, atherosclerotic plaques, myocardial infarction and fibrotic liver (Villalta et al., 2014; Foks et al., 2015; & Kaplan et al., 2016). Whether the tissue Treg populations described so far are unique or variants of the same population is unclear.

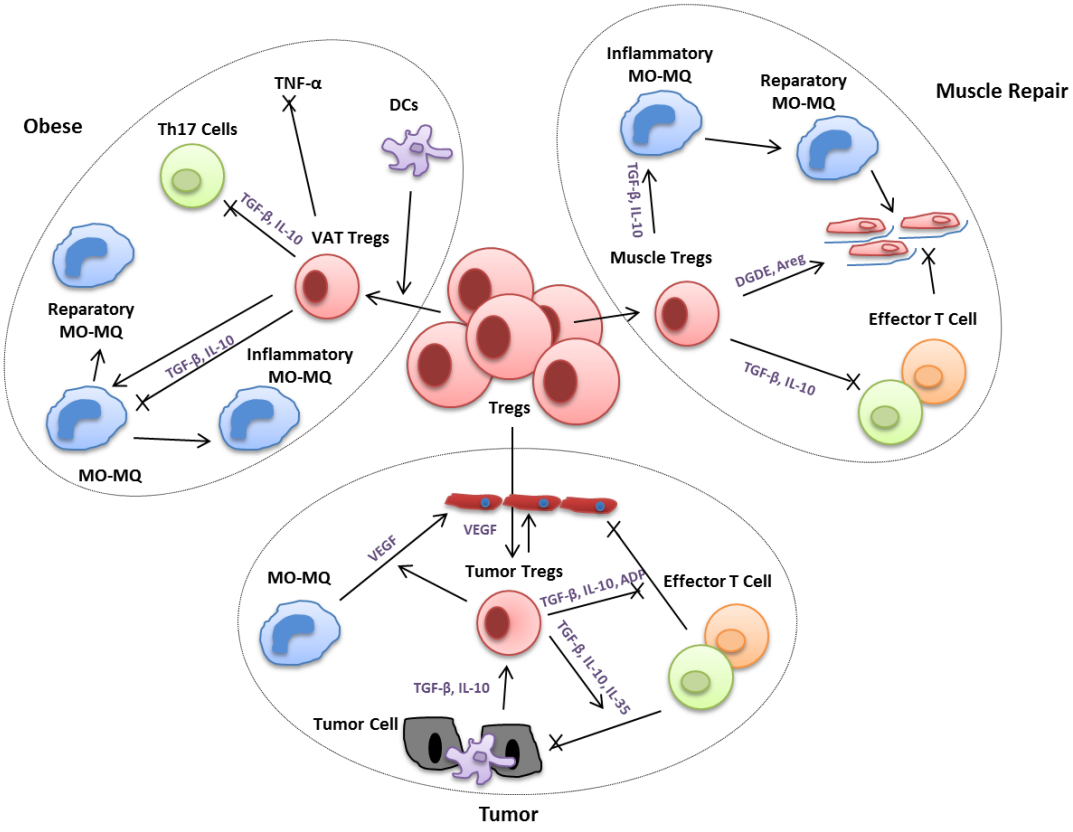


**Figure 1.5. Functions of tissue resident Treg cells in adipose tissue, muscle repair and tumour development.** (A) Treg cells suppress Th17 cells by secreting anti-inflammatory IL-10 and TGF-β and preventing the conversion of monocyte-macrophages. Alternatively, VAT Tregs directly attenuate the negative roles of TNF-α in inflammation in adipose tissue. (B) Muscle Treg cells modulate muscle repair through IL-10, CCR1, PGDF and amphiregulin (AREG). They hinder the transition of myeloid cells from a pro- to an anti-inflammatory phenotype and accelerate the differentiation of satellite cells, thereby promoting the regeneration of skeletal muscle. (C) Infiltrated Treg cells can promote tumour progression by inhibiting anti-tumour effector T cells via producing inhibitory cytokines. Treg cells also contribute to angiogenesis by enhancing VEGF production directly or through their effects on macrophages.

### 1.3. Aims of The Dissertation

Whether Treg cells play a role in venous thrombosis was completely unknown until now. Based on the observation that Tregs accumulate in venous thrombi, this dissertation was intended to clarify their functional role in thrombosis resolution. Projected steps included the selective manipulation of Treg numbers during thrombus resolution, the identification of possible Treg-dependent histological and cellular changes, the generation of an expression profile using RNA-Seq, and functional studies on Treg-produced factors.

# 2. MATERIALS AND METHODS

## 2.1. Materials

### 2.1.1. Laboratory Equipment

| Equipment | Manufacturer |
|---|---|
| Centrifuges | Thermo Fisher Scientific, Karlsruhe, Germany |
| BD LSR Flow Cytometer | Becton Dickinson, Heidelberg, Germany |
| Microscope | Leica, Wetzlar, Germany |
| Microtome | Leica, Wetzlar, Germany |
| Vevo 770 High-Resolution Imaging System | Visual- Sonics, Toronto, Canada |
| BD FACS ARIA II Cell Sorter | Becton Dickinson, Heidelberg, Germany |
| Qubit 2.0 | Invitrogen, Carlsbad, CA, USA |
| Bioanalyzer 2100 | Agilent Technolgies, Santa Clara, CA, USA |
| Thermal Cycler | Biorad, Hercules, CA, USA |
| Illumina HiSeq2500 | Illumina, San Diego, CA, USA |

Table 2.1.1. Instruments

### 2.1.2. Plastic Ware and Consumables

| Consumables | Manufacturer |
|---|---|
| 6-well cell culture plate | Costar, Bodenheim, Germany |
| 96-well cell culture plate | Costar, Bodenheim, Germany |
| Centrifuge tubes 15 ml / 50 ml tubes | Greiner GmbH, Frickenhausen, Germany |
| Disposable fine dosage syringes, 1 ml | Braun, Melsungen, Germany |
| Glass pipettes, 10 ml | Greiner, Frickenhausen, Germany |

| | |
|---|---|
| Pipette tips, 10 µl, 200 µl, 1000 µl | Greiner, Frickenhausen, Germany |
| Prolene sutures 6/0, 7/0 and 8/0 | Braun, Melsungen, Germany |
| Swab, wood/cotton | VWR, Cologne, Germany |
| Syringes 1 ml, 10 ml | Braun, Melsungen, Germany |
| Cell strainers 40 and 70 µm | Fisher Scientific, Schwerte, Germany |
| Magnetic stand-96 | Life technologies, Carlsbad, CA, USA |

Table 2.1.2. Plastic ware and consumables

### 2.1.3. Reagents, Kits, and Chemical Solutions

| **Reagents and solutions** | **Manufacturer** |
|---|---|
| AB-Diluent | Dako, CA, USA |
| Alzane 5 mg/ml | Zoetis, Berlin, Germany |
| BD Cytofix/Cytoperm kit | BD Bioscience, Heidelberg, Germany |
| BD FACS ™ Lysing Solution | BD Bioscience, Heidelberg, Germany |
| Bovine serum albumin (BSA) | PAA Laboratories, Pasching, Austria |
| Collagenase Type II | Life Technologies, Carlsbad, CA, USA |
| Depilatory cream Veet | Veet Reckitt Benckiser, Heidelberg, Germany |
| Diphtheria toxin (DT) | Merck, Darmstadt, Germany |
| DNase I | F. Hoffmann-La Roche, Basel, Switzerland |
| Dorbene Vet 1mg/ml | Zoetis, Berlin, Germany |
| Dulbecco phosphate buffer saline (DPBS) | Thermo Fisher Scientific, Karlsruhe, Germany |
| EDTA (Ethylenediaminetertraacetic acid) | Serva, Heidelberg, Germany |
| Entellan ® | Sigma-Aldrich, Steinheim, Germany |

| | |
|---|---|
| Ethanol 70% | Roth, Karlsruhe, Germany |
| Eye cream (Bepanthen®) | Bayer, Leverkusen, Germany |
| Fentanyl (0.05 mg/kg) | Janssen-Cilag, Neuss, Germany |
| Fetal bovine serum (FBS) | Thermo Fisher Scientific, Karlsruhe, Germany |
| Flumazenil Hikma (0,1 mg/ml) | Hikma, Gräfelfing, Germany |
| Formaldehyde | Roth, Karlsruhe, Germany |
| Gill's hematoxylin | Sigma-Aldrich, Steinheim, Germany |
| Hematoxylin | Roth, Karlsruhe, Germany |
| Heparin-Natrium-25000-ratiopharm | Ratiopharm GmbH, Ulm, Germany |
| Histo- Clear | Sigma-Aldrich, Steinheim, Germany |
| Human serum albumin (HAS) | Behring, Marburg, Germany |
| ImmoMount | Thermo Fisher Scientific, Karlsruhe, Germany |
| Isoflurane (Forene®) | Abbot, Wiesbaden, Germany |
| Isopropanol | Heidinger, Stuttgart, Germany |
| Mayer' s hematoxylin solution | Roth, Karlsruhe, Germany |
| Midazolam-hameln 5 mg/ml | Hameln Pharma, Hameln, Germany |
| NGS 10% (normal goat serum) | Abcam, Cambridge, UK |
| Orange G | Sigma-Aldrich, Steinheim, Germany |
| Paraffin | Roth, Karlsruhe, Germany |
| Peroxidase substrate (AEC) | VectorLabs, CA, USA |
| Phosphoric acid | Roth, Karlsruhe, Germany |
| Poly-lysine coated glass slides | Sigma-Aldrich, Steinheim, Germany |
| Ponceau-Scarlett | Sigma-Aldrich, Steinheim, Germany |
| Roti-liquid barrier | Roth, Karlsruhe, Germany |

| | |
|---|---|
| Saturated picric acid | Sigma-Aldrich, Steinheim, Germany |
| Sirus red | Sigma-Aldrich, Steinheim, Germany |
| Sodium chloride (NaCl) | Roth, Karlsruhe, Germany |
| Temgesic ampullen 0.3 mg | RB Pharmaceuticals Limited, United Kingdom |
| Vectastain ABC kit | VectorLabs, CA, USA |
| Zinc formalin fixative | Sigma-Aldrich, Steinheim, Germany |
| Mouse IL-2 recombinant protein carrier-free | eBioscience, MA, USA |
| MMP Sense ™ 645 FAST | Pekrin Elmer, Boston, USA |
| Qubit 2.0 dsDNA high sensivity assay kit | Agilent Technologies, Sta. Clara, CA, USA |
| Nuclease-free water | Qiagen, Hilden, Deutschland |
| Nextra XT DNA sample preparation kit | Illumina, San Diego, CA, USA |
| Nextra index primer | Illumina, San Diego, CA, USA |
| Ampure XP beads kit | Beckman Coulter, Brea, CA USA |
| High-sensivity DNA chip | Agilent Technologies, Sta. Clara, CA, USA |
| SMART-Seq v4 ultra low input RNA kit | BioLab, Frankfurt am Main, Germany |
| MiSeq® Reagent kit v2 (50 Zyklen) | Illumina, San Diego, CA, USA |

Table 2.1.3. Reagents, kits, and chemical solutions

### 2.1.4. Surgical Instruments

| **Instrument** | **Manufacturer** |
|---|---|
| Forceps | 0.2 mm medicon® Micro-Forceps, Tuttlingen, Germany |
| Halsted-mosquito hemostat | Fine Science Tools GmbH, Heidelberg, Germany |
| Surgical scissors 14 cm | Fine Science Tools, San Mateo, CA, USA |

Table 2.1.4. Surgical instruments

### 2.1.5. Antibodies

| Antibody | Clone | Isotype | Manufacturer |
|---|---|---|---|
| CD115 (CSF-1R) | AFS98 | Rat IgG2a, kappa | BioLegend, San Diego, USA |
| CD11b | M1/70.15 | Rat IgG2b | BD Pharmingen, San Jose, USA |
| CD11c | N418 | Armenian Hamster IgG | BioLegend, San Diego, USA |
| CD183 (CXCR3) | CXCR3-173 | Armenian Hamster IgG | BioLegend, San Diego, USA |
| CD3 | 17A2 | Rat (SD) IgG2b, kappa | BD Pharmingen, San Jose, USA |
| CD335 (NKp46) | 29A1.4 | Rat IgG2a, kappa | BioLegend, San Diego, USA |
| CD4 | GK1.5 | Rat IgG2b, kappa | eBioscience, MA, USA |
| CD45 | 30-F11 | Rat IgG2a, kappa | BioLegend, San Diego, USA |
| CD62L (L-Selectin) | MEL-14 | Rat IgG2a, kappa | eBioscience, MA, USA |
| CD69 | H1.2F3 | Armenian Hamster IgG | eBioscience, MA, USA |
| F4/80 | BM8 | RatIgG2a, kappa | eBioscience, MA, USA |
| Foxp3 | FJK-16s | RatIgG2a, kappa | eBioscience, MA, USA |
| Helios | 22F6 | Armenian Hamster IgG | Biolegend, San Diego, USA |
| I-A/I-E | M5/114.15.2 | Rat IgG2b, kappa | BioLegend, San Diego, USA |
| Ki-67 | SolA15 | Rat IgG2a, kappa | eBioscience, MA, USA |
| KLRG1 (MAFA) | 2F1/KLRG1 | Golden Syrian Hamster IgG | eBioscience, MA, USA |
| Ly-6C | HK1.4 | Rat IgG2c, kappa | eBioscience, MA, USA |
| Ly-6G | 1A8 | Rat IgG2a, kappa | BioLegend, San Diego, USA |
| NK-1.1 | PK136 | Mouse IgG2a, kappa | BioLegend, San Diego, USA |
| T-bet | eBio4B10 | Mouse IgG1, kappa | eBioscience, MA, USA |
| TCR beta Chain | H57-597 | Armenian Hamster IgG2 | BD Pharmingen, San Jose, USA |
| CD25 | PC61.5 | Rat IgG2a, kappa | BioLegend, San Diego, USA |

| | | | |
|---|---|---|---|
| IL-2 (JES6-1A12) | JES6-1A12 | Rat IgG2a, kappa | BioLegend, San Diego, USA |
| α-SMA | 1A4 | Mouse IgG2a, kappa | Sigma, St. Louis, MO, USA |
| CD31 | SZ31 | Rat IgG2a | Dianova, Hamburg, Germany |
| Mac2 (Galectin-3) | M3/38 | Rat IgG2a | Biozol, Eching, Germany |
| F4/80 | A3-1 | Rat IgG2a | Bio-Rad, CA, USA |
| Biotin-Conjugated Goat Anti-Rat IgG | Polyclonal | Polyclonal | Thermo Fisher Scientific, Karlsruhe, Germany |
| Amphiregulin Biotinlated | Polyclonal | Polyclonal IgG | R&D Systems, Minneapolis, USA |
| ST2 (IL-1rl1) | DIH9 | Rat IgG2a | BioLegend, San Diego, USA |
| CD218a (IL-18R) | | Rat IgG2a | BioLegend, San Diego, USA |

Table 2.1.5. Antibodies

### 2.1.6. Buffers

| **Buffer** | **Instruction** |
|---|---|
| Acetic acid (30%) | 120 ml 100% acetic acid, 280 ml dH2O |
| ACK-buffer | 0.15 M $NH_4Cl$, 1 mM $KHCO_3$, 0.5 mM EDTA, pH 7.2 |
| Aniline blue solution (1%) | 2 g aniline blue, 200 ml 1% acetic acid |
| Bouin solution | 750 ml saturated picric acid, 250 ml formaldehyde, 50 ml picric acid |
| Citrate buffer 0.01 M (pH 6.0) | 100 ml 0.01 M citrate buffer, 900 ml dH2O |
| FACS-buffer | 1xPBS, 0.5% human albumin, 1mM EDTA, 10 µg/ml IVIg |
| Ferric ammonium sulphate solution (5%) | 10 g ferric ammonium sulphate, 200 ml $dH_2O$ |
| $H_2O_2$ (3%) | 450 ml methanol, 50 ml 30% $H_2O_2$ |
| Normal goat serum 10% (NGS) | 500 µl normal goat serum, 4500 µl PBS |
| PBS 10X | 80.4 g NaCl, 15.6 g $NaH_2PO_4$ x 2 $H_20$, pH 6.6 |

| | |
|---|---|
| Phosphotungstic acid (1%) | 2.5 g phosphotungstic acid, 250 ml $dH_2O$ |
| Picric acid-orange G solution | 200 ml saturated picric acid, 4 g Orange G |
| Ponceau-puchsin solution | 1 g acid fuchsin, 1 g Ponceau 2R, 200 ml 1% acetic acid |
| Sirius red solution | 1 g sirius red, 100 ml saturated picric acid |

Table 2.1.6. Buffers

### 2.1.7. Experimental Animals

| Strain | Source | Official Strain Name | Stock Number |
|---|---|---|---|
| C57BL/6J | Jackson Laboratory, ME, USA | C57BL/6J | 000664 |
| Nur77$^{GFP}$ | Jackson Laboratory, ME, USA | C57BL/6-Tg(Nr4a1-EGFP/cre)820Khog/J | 016617 |
| DEREG | Jackson Laboratory, ME, USA | 57BL/6-Tg(Foxp3-DTR/EGFP)23.2Spar/Mmjax | 32050-JAX |
| KLF-2 $^{GFP}$ | Jackson Laboratory, ME, USA | B6;129S4-Klf2tm1.1Hhn/J | 026926 |

Table 2.1.7. Experimental animals

### 2.1.8. Software

| Software | Manufacturer |
|---|---|
| Image ProPlus, version 7.0 | Media Cybernetics Image, Washington, USA |
| BD FACSDiva software 7.0 | Becton Dickinson, Mountain View, CA, USA |
| GraphPad prism version 7.0 | Graphpad Software, Inc., La Jolla, Ca, USA |
| FlowJo version 10.0 | Tree Star, Inc, Ashland, OR, USA |

Table 2.1.8. Software

## 2.2. Methods

### 2.2.1. Mice

All mice were bred in the central animal facility of the Johannes Gutenberg University Mainz. All animal experiments were performed in accordance with animal laws, current institutional guidelines, and in compliance with national guidelines for the care and use of laboratory animals.

**C57BL/6J wild type (WT) Mice:** C57BL/6J mice are a common inbred strain, widely used as the genetic background for genetically modified mice.

**DEREG Mice:** DEREG (Depletion of Regulatory T Cells) mice. These mice express a simian diphtheria toxin receptor-enhanced green fluorescent protein (DTR-eGFP) fusion protein under the control of the endogenous forkhead box P3 (Foxp3) promoter/enhancer regions on a BAC (bacterial artificial chromosome) transgene. Foxp3$^{+}$ Treg can thus be tracked in these mice by their GFP expression and selectively eliminated by diphtheria toxin (DT) injection (Lahl et al., 2011).

**KLF2-GFP Mice:** KLF2-GFP knock-in mice were generated by inserting the GFP gene in-frame at the KLF2 translational start site of exon 1 and thus created a GFP-KLF2 fusion protein that allows the monitoring of KLF2 expression in cells (Takada et al., 2011).

**Nur77-GFP Mice:** To create a fluorescent reporter that would be activated by TCR signalling in T cells, a GFP-Cre fusion protein was inserted at the start codon of the Nr4a1 (Nur77) gene in a BAC.

### 2.2.2. DVT Induction by Flow Reduction in the Interior Vena Cava (IVC Ligation Model)

**Principal:** Partial flow restriction in the IVC mimics the conditions found at in human venous valves and results in the formation of thrombi similar in structure to human thrombi.

**Procedure:** DVT was induced in 8-12 week old mice with a minimum body weight of 25 grams by ligation of the IVC and all visible tributaries. Animals were placed in an anaesthesia chamber and sedated by 2.5% isoflurane (flow rate 0.8 litres/minute). Mice were subsequently anaesthetised with an intraperitoneal (i.p.) injection of Midazolame (5 mg/kg), Dorbene Vet (1 mg/ml), and Fentanyl (0.05 mg/kg). The abdomen was shaved with a hair epilator. Animals received eye lubrication and supplemental thermal support during anaesthesia.

| Medication (stock concentration) | Injected Concentration |
|---|---|
| Dorbene (1 mg/ml) | 15 $\mu$g/kg |
| Midazolam (5 mg/kg) | 0.15 mg/kg |
| Fentanyl (0.05 mg/kg) | 0.15 $\mu$g/kg |
| NaCl (0.9%) | 15 $\mu$g/kg |

**Table 2.2.1.** Anaesthesia cocktail

Surgery was started by making a midline incision (2 cm) through the skin and abdominal wall. A moistened gauze pad was used to move the small intestines to the animal's left side. Mice were then restrained to allow for the visualisation of the IVC. A 6-0 Prolene suture was placed longitudinally along the ventral surface of the IVC, and the infrarenal IVC was ligated with 8-0 non-reactive Prolene suture. The 6-0 Prolene suture was then removed, allowing blood flow to return. The laparotomy site was fastened in a two-layer manner with 7-0 non-reactive Prolene.

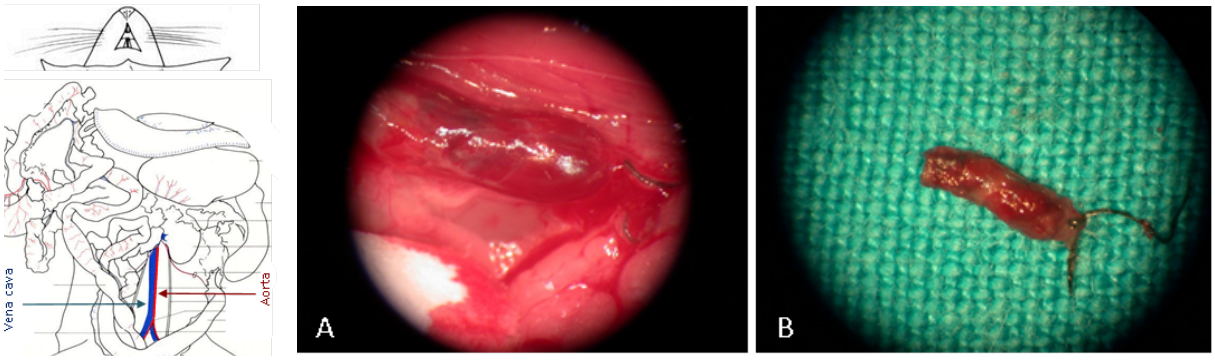


**Figure 2.2.1. Schematic representation of the inferior vena cava (IVC) stenosis models.** Left) anatomic position of the IVC. A) and B) Ligated IVC in place and upon explantation (Pictures kindly provided by Lucas Hobohm).

After ligation, mice were antagonised with a subcutaneous (s.c.) injection of Flumazenil (0.1 mg/kg), Alzane (5 mg/kg) and Temgesic (0.324 mg/ml) as a post-operative analgesic, which does not interfere with the study's objective. To prevent infections, ligated mice received Borgal (1 mg/mL sulfadoxin and 0.2 mg/mL trimethoprim) in their drinking water (Brandt et al., 2012).

| Medication (Stock concentration) | Injected Concentration |
|---|---|
| Flumazenil (1 mg/ml) | 15 $\mu$g/kg |
| Alzane (5 mg/kg) | 75 $\mu$g/kg |
| NaCl (0.9%) | 15 $\mu$g/kg |

**Table 2.2.2.** Antagonist cocktail

At different time points, ligated mice were anaesthetised using isoflurane and killed by exsanguination. Blood samples were collected by right ventricular puncture, and the vessel system was flushed with 15 ml of 1X phosphate-buffered saline (PBS). 100 µl Heparin per 1 ml blood was used as an anticoagulant agent. The IVC was excised caudal to the ligation. Upon the removal of perivascular fat, the vein was opened longitudinally, and the thrombus dissected. The luminal surface was gently scraped to remove attaching blood-born cells.

### 2.2.3. High Frequency Ultra Sound Measurement (HFUS)

**Principal:** Thrombus sizes were monitored non-invasively by high frequency ultrasound (HFUS) imaging (Vevo770 system) using a 40 MHz frequency mouse scan head. HFUS is an effective method for real-time imaging of thrombus development (Aghourian et al., 2013). Thrombi are identified in transverse and longitudinal planes due to their hyper-echoic nature compared with surrounding blood.

**Procedure:** Mice were sedated by mask inhalation of 2.5% vaporised isoflurane (0.25 litres per minute (L/min) $O_2$) and kept anaesthetised with 0.5- 1.5% isoflurane (0.05-0.1 L/min$O_2$) on a 37° C heating plate during observation. Ultrasound transmission gel was applied to the shaved abdomen to improve sound transmission/

recording. A long axis view was applied to visualise the IVC, the ligation site, and the formed thrombus in place. The PW doppler mode can be used to display the movement of the corpuscular components in blood, their direction, and flow rate. This aids in precise ultrasound head positioning by distinguishing venous from adjacent arterial blood flow. Upon optimal transverse and longitudinal positioning of the ultrasound head a freeze-frame image was taken manually and the cross-sectional area of the clot traced using the Vevo 770 software. The length and width of clots were additionally measured by applying B-mode (Brandt et al., 2012).

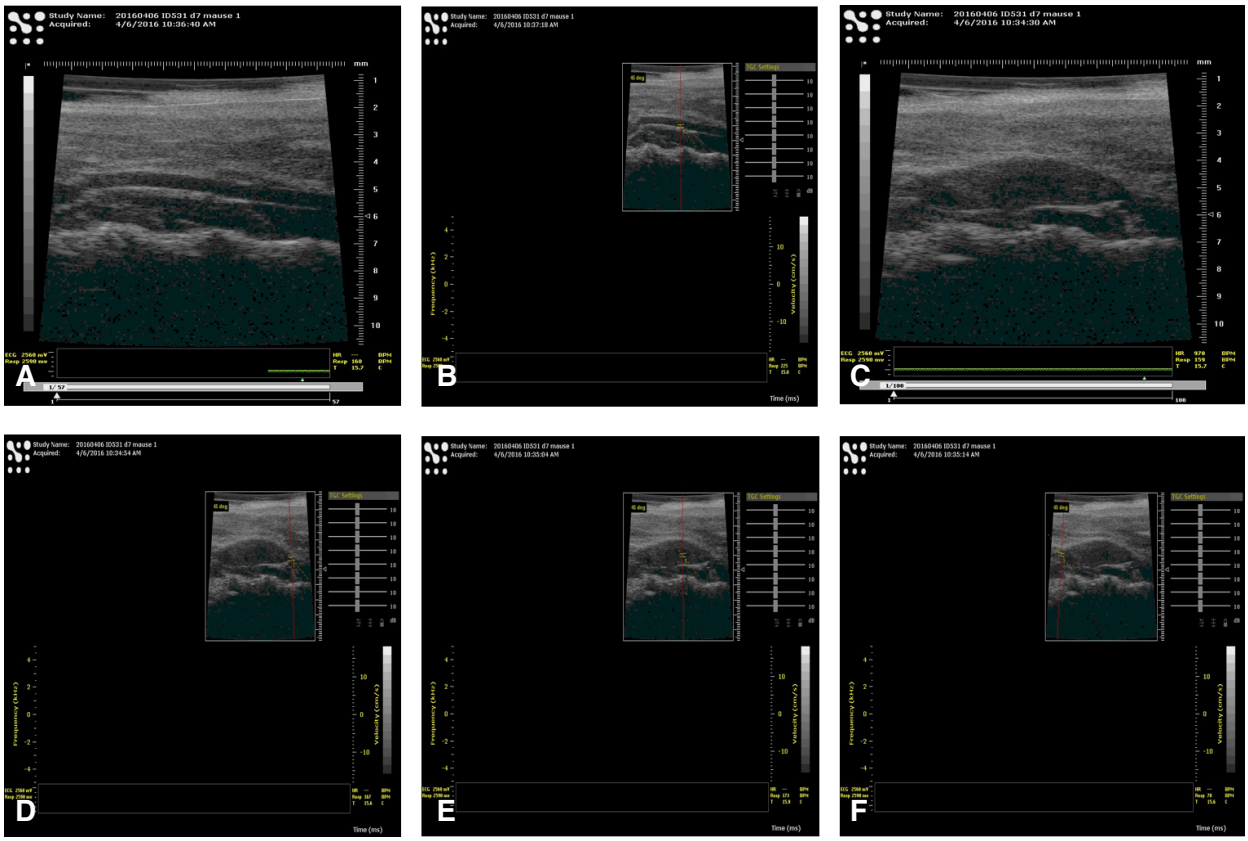


**Figure 2.2.2. Monitoring of inferior vena cava (IVC) thrombi with high-frequency ultrasound (HFUS).** (A and B) Aorta visualisation to distinguish from IVC adjacent to each other in ligated mice. (C) Representative image of the IVC in axial view of the thrombus and vein 14 days after DVT induction. (D, E and F) HFUS also allows quantification of blood flow velocity and thrombus presence. Using the pulse-wave Doppler function no flow was observed in the ligated group.


**Figure 2.2.3. Longitudinal thrombus resolution quantified by HFUS.** Left: Representative visualisation of a venous thrombus by HFUS. Right: Representative longitudinal HFUS-based representation resolving IVC thrombi in C57Bl/6J mice overtime.

### 2.2.4. Tregs Depletion by Diphtheria Toxin Injection in DEREG Mice

**Principal:** DEREG mice express a simian diphtheria toxin receptor-enhanced green fluorescent protein (DTR-eGFP) fusion protein that is under the control of the endogenous forkhead box P3 (Foxp3) promoter/enhancer regions on a BAC (bacterial artificial chromosome) transgene. Injection of diphtheria toxin selectively depletes Tregs (Lahl et al., 2011).

**Procedure:** For depletion, DT doses below the total concentration leading to renal damage were administered. 1 mg of diphtheria toxin was reconstituted in 1 ml of sterile PBS and aliquoted into 100 ml stocks. Each vial was later diluted with sterile PBS to provide 10 ml of 1 mg DT/100 ml PBS working stock. DEREG mice received two injections of 1 mg DT (500 µl) i.p. for two consecutive days (day 8 and 9 after DVT) and Treg cell depletion was monitored by flow cytometry (Mayer et al., 2014).

### 2.2.5. Treg Expansion by IL-2/anti-IL-2 Complexes

**Principal:** It is known that IL-2 bound to the neutralising IL-2 specific monoclonal antibody JES6-1, actively induces the expansion and activation of IL-2Rα$^{hi}$ (CD25$^{hi}$) cells, preferentially expanding Treg cells over effector T cells (Boyman et al., 2006).

**Procedure:** For the expansion of Tregs, we incubated 5 µg anti-mouse IL-2 monoclonal antibody (mAb) (JES6-1) and 1.5 µg mrIL-2 per mouse for 30 min on ice. For Treg expansion mice were injected i.p. each day for 4 days with a final volume of

200 µl IL-2/JES6-1. Control mice were administered PBS (Webster et al., 2009; & Létourneau et al., 2010).

### 2.2.6. Flow Cytometry

**Principle:** Flow cytometry provides a unique technique to distinguish heterogeneous cell types based on protein expression differences. This method specifically allows the detection and identification of multiple cell surface, intracellular or intra-nuclear target proteins in single cells simultaneously.

In addition, light scattering at distinctive angles can distinguish differences in size and complexity. Different lasers emit monochromatic light of distinct wavelengths that excite cell-bound fluorochromes (such as by bound fluorochrome-labelled antibodies) and are detected by individual detectors.

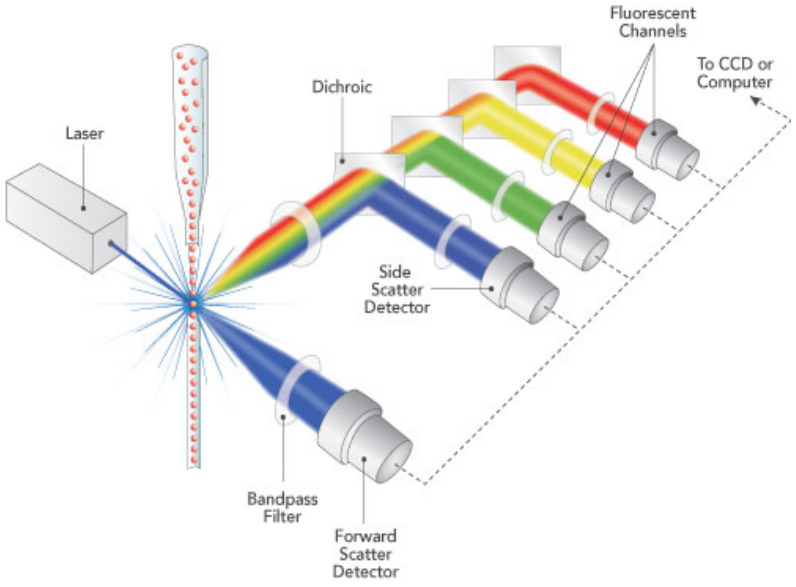


**Figure 2.2.4. Schematic representation of a flow cytometer.** A single cell suspension is hydrodynamically generated with sheath fluid to cross an argon-ion laser beam. Signals are simultaneously collected by a forward light scatter detector, a side-scatter detector, and multiple fluorescence emission detectors.

### 2.2.6.1. Fluorochromes

| Fluorochrome | Abbreviation | Absorption peak [nm] | Emission peak [nm] |
|---|---|---|---|
| Allophycocyanine | APC | 650 | 660 |
| Allophycocyanine-Cyanine 7 | APC-Cy7 | 650 | 767 |
| AmCyan | - | 457 | 491 |
| Fluoresceinisothiocyanate | FITC | 495 | 520 |
| Fixable Viability Dye eFluor 780 | Fix Dye | 633 | 780 |
| Pacific Blue | PB | 405 | 456 |
| Peridinin chlorophyll-Cyanine | PerCP-Cy5.5 | 490 | 677 |
| R-Phycoerythrin | PE | 495 | 576 |
| R-Phycoerythrin-Cyanine 5 | PE-Cy5 | 495 | 696 |
| R-Phycoerythrin-Cyanine 7 | Pe-Cy7 | 495 | 767 |

**Table 2.2.3. Fluorochromes used on flow cytometry antibodies.** Each fluorophore has a characteristic peak excitation and emission wavelength.

### 2.2.6.2. Cell Preparation

Isolated lymphoid organs were separated to generate single cell suspensions by pressing them with the plunger of a 3 ml syringe through a 70 µ mesh. Mouse IVCs were cut into small pieces and lysed for 15 min at 37°C using a mixture of DNAse I (50 µg/ml) and collagenase type II (1 mg/ml). The digestion procedure did not affect any of the markers used. Upon resuspension in 10 ml flow cytometry staining buffer, the cell suspension was passed through a cell strainer to eliminate clumps and debris. The resulting single cell suspensions were transferred into 15-ml falcon tubes and centrifuged for 10 min at 360 *g*, 4°C. In order to remove red blood cells, 1-3 ml ACK buffer was added to cell pellets for 2 min.

#### 2.2.6.3. Cell Surface Staining

To analyse the expression of cell surface molecules, cells were seeded with a density of $1x10^5$-$1x10^6$ cells/per well into individual wells of a 96-well plate, washed twice with FACS buffer and pelleted by centrifugation at 360 *g* for 10 min at 4 °C. Next, cells were resuspended in a defined volume of staining buffer and incubated with unlabelled mAb against CD16/CD32 to block nonspecific Fc receptor-mediated binding of staining antibodies used in the subsequent staining. Cells were then stained with fluorochrome-conjugated antibodies for 30 min at 4° C. After two washing steps performed to remove unbound antibodies, cells were resuspended in 200 µl FACS buffer.

#### 2.2.6.4. Staining Intracellular (nuclear) Targets

For intracellular molecule expression analysis, cells were incubated in 100 µl Fixation/Permeabilisation working solution (1 x Fixation/Permeabilisation Concentrate with 3x Fixation/Permeabilisation Diluent) for 30 min at room temperature (RT) after the cell surface staining was completed. Subsequently, cells were washed twice with 1 x Permeabilisation Buffer (mixing 1 part of 10X concentrate with 9 parts distilled water), and stained with the corresponding mAb for 30 min at RT. After 2 more washings with Permeabilisation Buffer, pellets were resuspended in 200 µl FACS buffer.

#### 2.2.6.5. Matrix Metalloproteinase (MMP) Activity Probing

MMP Sense is a MMP-activated probe that is optically silent upon injection and produces a fluorescent signal after cleavage by MMPs. Activation occurs by a broad range of MMPs including MMP 2, 3, 7, 9, 12, and 13. To analyse MMP activity in individual immune cells in thrombus resolution, 100 µl (4 nmol) of PBS-reconstituted MMP Sense 645 was injected intravenously (i.v.) and the retrieved organs flow cytometrically analysed 24 hours later.

#### 2.2.6.6. In vitro Amphiregulin Production

For the analysis of amphiregulin (AREG) production from Tregs, ex vivo isolated cells from spleen and thrombus were isolated and stimulated, with IL-18 ( ng/ml) and IL-33 (ng/ml) for 4 hours in the presence of marimastat (10 mM, Sigma), GolgiPlug (brefeldin A) and GolgiStop (monensin) and stained directly.

#### 2.2.6.7. Flow Cytometric Analyses

All flow cytometry measurements were performed on a BD LSR II cytometer. Flow Jo Version 8.8.7 was used for data analysis.

### 2.2.7. Histological Analyses

Thrombotic tissue samples (IVC and thrombi) were collected, fixed in 4% zinc formalin, and then embedded in paraffin. For further histological analysis, 4 µm-thick serial sections were cut over the IVC segment and 5 longitudinal sections were stained and investigated on average.

#### 2.2.7.1. Carstairs Staining

**Principal:** Carstairs staining allows to differentiation between fibrin (bright red), collagen (bright blue), muscle cells (red), and erythrocytes (yellow-orange).

**Procedure:** Paraffin embedded sections were de-waxed using xylol and rehydrated through a descending row of alcohols (100%, 70% and 50% EtOH). The slides were incubated for 1 h in Bouin's fixative at 60°C. Next, they were rinsed with $dH_2O$ and stained in a 5% ferric ammonium sulphate solution. The slides were washed again and stained with Mayer's hematoxylin. After rinsing with tap water, picric acid-orange G solution was applied to detect erythrocytes. The slides were rinsed with $dH_2O$ and the muscle cells were then dyed red using Ponceau-Fuchsin solution. A 1% phosphotungstic acid solution was used to destain the connective tissue, and collagen fibres were stained using a 1% aniline blue solution. The sections were

dehydrated with an ascending ethanol gradient (95%, 100% EtOH) and rinsed with histo-clear solution (equal to xylol) to embed the stained sections with Entellan® as a mounting medium.

#### 2.2.7.2. Sirius Red Staining

**Principal:** Interstitial collagen was detected using Sirius red staining followed by polarisation microscopy. Sirius red staining is considered a highly specific staining that differentiates collagen types. The larger collagen fibres stain bright red or orange whereas the thinner ones appear yellow.

**Procedure:** Paraffin embedded sections were de-waxed using xylol and rehydrated through a descending row of alcohols (100%, 96%, 70%, and 50% EtOH). The slides were stained in 1% Picro-Sirius red for one hour, then washed in two changes of 30% acetic acid. The sections were dehydrated in 100% ethanol and cleared in Roti-clear solution (equal to xylol) to mount in Entellan®.

#### 2.2.7.3. Immunohistochemistry

**Principal:** The structural and cellular composition of specimens was examined using immunohistochemistry.

**CD31 (PECAM-1):** CD31 is one of the major markers that indicates the presence of endothelial cells and thus a determinant of venous thrombus resolution and neovascularisation (Lertkiatmongkol et al., 2016).

**Alpha-smooth muscle actin (α-SMA):** Myofibroblasts were identified by expression of α-SMA. Myofibroblasts are considered to be the key activated fibrinogenic cells in normal wound repair, and α-SMA is used as a marker for myofibroblast proliferation and activated tissue fibrinogenic cells (Hinz et al., 2001).

**F4/80:** F4/80 is a glycoprotein with 80% surface membrane expression, which is specifically expressed in tissue macrophages.

**MAC2 (Galectin 3):** MAC2 or galactose-specific lectin 3 is an intracellular protein associated with the maturation of a subset of monocytes/macrophages during

inflammation. Mac-$2^+$ macrophages have a key role in tissue repair, debris scavenging, and angiogenesis. In response to inflammation and tissue repair, F4/$80^+$ Mac-$2^+$ macrophages can be identified in inflamed tissue.

**Procedure:** Paraffin embedded sections were deparaffinised using xylol and rehydrated through a descending row of alcohols (100%, 96%, 70%, and 50% EtOH) and then quenched in methanol- 3% $H_2O_2$ for endogenous peroxidase activity. For heat induced-epitope retrieval, 0.01 M citrate buffer was used for 11 min. The blocking of unspecific antigen binding sites was done with 10% normal goat serum. Endothelial cells, smooth muscle cells, and macrophages were visualised using monoclonal antibodies against murine CD31 (dilution, 1:20), SMA (dilution, 1:800), F4/80 (dilution, 1:200) or Mac2 (dilution, 1:400) overnight at 4°C, respectively, followed by incubation with a biotin-conjugated goat anti-rat IgG antibody (dilution, 1:1000) for 60 min at RT, avidin biotin link (Vectastain ABC kit) for 30 min and peroxidase substrate (AEC) for 10 min. Sections were briefly counterstained with Gill's hematoxylin and then mounted with ImmoMount. Negative controls, after the exclusion of the first antibody and incubation with secondary anti-mouse or anti-rabbit antibodies alone, were run in parallel.

#### 2.2.7.4. Pictures

All pictures were recorded with an Olympus BX51 microscope. Marker expression was automatically quantified by defining positive areas per total tissue area. All morphometric analyses were performed using Image ProPlus analysis software.

### 2.2.8. Next-Generation Sequencing (NGS)

**Principal:** Next-generation sequencing (NGS), also known as high-throughput sequencing, provides sequencing of millions of small fragments of DNA in parallel from the whole genome. Through this large-scale sequencing, we are able to obtain cDNA libraries from small cell numbers and perform transcription analysis.

#### 2.2.8.1. Flow Cytometry- Based Isolation of Regulatory T Cells

The mouse IVCs were prepared following as per section 2.2.6.2. Cells were then stained with fluorochrome-conjugated antibodies for 30 min at 4°C. $CD45^+$ $CD4^+$ $CD69^+$ $Foxp3^+$ cells were separated with FACS Sorter.

#### 2.2.8.2. Generation of Full-Length cDNA

##### 2.2.8.2.1. First-Strand cDNA Synthesis

The first-strand cDNA synthesis (from total RNA or cells) was primed by the 3' SMART-Seq CDS Primer II A and used the SMART-Seq v4 Oligonucleotide for template switching at the 5' end of the transcript. The cells collected from sorting were diluted in 8.5 µl nuclease-free water and 1µl reaction buffer. 2 µl of 3' SMART-Seq CDS Primer II A (12 µM) was added and the tubes were incubated at 72°C in a preheated, hot-lid thermal cycler for 3 min. The master mix was prepared following reagents in the order of Table 2.2.4. 7.5 µl of the master mix was added to each reaction tube and then following program was run (Table 2.2.5):

| | | |
|---|---|---|
| 17 cycles: | 95°C | 1 min |
| | 98°C | 10 sec |
| | 65°C | 30 sec |
| | 68°C | 3 min |
| | 72°C | 10 min |
| | 4°C | forever |

**Table 2.2.4. Master mix component for first-strand cDNA synthesis.**

| | |
|---|---|
| 4 µl | 5X Ultra Low First-Strand Buffer |
| 1 µl | SMART-Seq v4 Oligonucleotide (48 µM) |
| 0.5 µl | RNase Inhibitor (40 U/µl) |
| 2 µl | SMARTScribe Reverse Transcriptase |

**Table 2.2.5. PCR program for first-strand cDNA synthesis.**

#### 2.2.8.2.2. cDNA Amplification by PCR

30 µl of PCR Master mix (Table 2.2.6) were added to each tube containing 20 µl of first-strand cDNA product from the previous step and then the following program was run (Table 2.2.7):

| | |
|---|---|
| 25 µl | 2X SeqAmp PCR Buffer |
| 1 µl | PCR Primer II A (12 µM) |
| 1 µl | SeqAmp DNA Polymerase |
| 3 µl | Nuclease-Free water |

**Table 2.2.6. Master mix components for cDNA amplification.**

| | |
|---|---|
| 42°C | 90 min |
| 70°C | 10 min |
| 4°C | forever |

**Table 2.2.7. PCR program for cDNA amplification.**

#### 2.2.8.2.3. Purification of Amplified cDNA

1 µl of 10X Lysis Buffer and 50 µl of AMPure XP beads were added to each PCR product then incubated at RT for 8 min to let the cDNA bind to the beads. The samples were placed on the magnetic separation device for 5 min until the liquid appeared completely clear and then the supernatant was discarded. 200 µl of freshly made 80% ethanol was added to each sample.

The samples were placed on the magnetic separation device one more for 30 seconds to remove all the remaining ethanol. The dried beads were eluted with 17 µl of elution buffer (EB) to rehydrate. The sample were placed back on the magnetic separation device for 1 min and clear supernatant containing purified cDNA was transferred to a nuclease-free tube to be analysed further.

#### 2.2.2.8.4. Total cDNA Quality and Concentration Assessment

The accurate quantification of cDNA was measured with the Qubit HS DNA assay kit. 1 µl of Qubit DNA HS reagent were diluted in 199 µl DNA HS buffer (working solution), then 2 µl eluted DNA was added to were transferred in 198 µl working solution. After 2 min of incubation in RT, the samples were measured.

### 2.2.8.3. Determining the Concentration of Full-Length cDNA

The quality and concentration of etude DNA was checked on the Bioanalyzer 2100 using a DNA high sensitive chip.15 µl HS DNA dye was added to a HS DNA gel matrix vial. 5 µl of marker was added into all sample wells and in the ladder well. Afterwards 1 µl of DNA sample was pipetted into each sample well and the chip was run on the bioanalyzer 2100.

| Sample | From (pb) | To (bp) | Average Size | Conc. (pg/ul) | Molarity (pmol/l) |
|---|---|---|---|---|---|
| Thromus | 69 | 7,549 | 573 | 4,695.36 | 18,524.2 |
| Spleen | 200 | 1,000 | 473 | 5,211.24 | 21,052.2 |

**Table 2.2.7. Library size distributions full-length cDNA.**

### 2.2.8.4. Preparation of Sequencing Library

#### 2.2.8.4.1. Tagment Genomic DNA

5 µl ATM, 10 µl TD and 5 µl normalised input DNA were mixed and centrifuged at 280 × *g* at 20°C for 1 min then placed in a thermal cycler and run at 55°C for 5 min, and held at 10°C. 5 µl NT was added and incubated at RT for 5 min.

#### 2.2.8.4.2. Library Amplification

25 µl enrichment PCR product, 15 µl NPM, 5 µl Index primer I (N7XX) and 5 µl Index primer II (N5XX) were mixed into each well and the PCR program was run as per Table 2.2.8.

| | | |
|---|---|---|
| | 72°C | 3 min |
| 12 cycles: | 95°C | 30 sec |
| | 95°C | 10 sec |
| | 55°C | 30 sec |
| | 72°C | 30 sec |
| | 72°C | 5 min |
| | 10°C | forever |

**Table 2.2.8.** PCR program for library amplification.

#### 2.2.8.4.3. Cleaning The Libraries

30 µl AMPure XP beads were added to 50 µl PCR product from each well of the PCR plate and incubated at RT for 5 min on a magnetic stand. 200 µl fresh 80% EtOH was added to each well on the magnetic stand for 30 seconds then the supernatant from each well was discarded. 52.5 µl RSB was added to air-dry the samples which were then and incubated for 2 min. 50 µl supernatant was transferred to a new PCR plate.

#### 2.2.8.4.4. Checking the Concentration of Final cDNA Libraries

1 µl of undiluted library was run on an Agilent Technology 2100 Bioanalyzer using a high sensitivity DNA chip.

#### 2.2.8.4.5. Pooling The Libraries

Pooling libraries combines equal volumes of normalised libraries in a single tube. After pooling, the library pool was diluted and heat-denatured before loading the libraries for the sequencing run.

#### 2.2.8.4.6. DNA Sequencing

Barcoded RNA-Seq libraries were onboard clustered using HiSeq® Rapid SR Cluster Kit v2 using 8pM and 59bps were sequenced on the Illumina HiSeq2500 using HiSeq® Rapid SBS Kit v2 (59 Cycle). The raw output data of the HiSeq was preprocessed according to the Illumina standard protocol. Sequence readings were trimmed for adapter sequences and further processed using the software CLC

Genomics Workbench (v7.5.1 with CLC's default settings for RNA-Seq analysis). Readings were aligned to the GRCm38 genome.

### 2.2.9. Statistical Analysis

Quantitative data are presented as mean± SEM. Differences were tested by Student t-test for unpaired means if normally distributed, or Mann–Whitney test if not normally distributed. Differences between multiple groups were compared using the 1-way ANOVA analysis of variance. Statistical significance was assumed if the P value was $<0.05$. All analyses were performed using GraphPad PRISM 7 data analysis software.

# 3. RESULTS

## 3.1. Treg Recruitment to The Thrombus and Vein Wall

Venous thrombus formation and resolution takes place in four phases: 1) hemostasis 2) inflammation 3) proliferation and 4) remodelling. Upon activation of the endothelium and clotting immune cells actively enter the thrombus and vein wall. The first wave of responder cells consists of neutrophils, and this is subsequently followed by monocytes and T cells (Branchford et al., 2018). Investigating the composition of the T cell infiltrate in thrombotic veins compared to blood and lymphoid tissue over time, we observed that Treg cells accumulate in the thrombus and vein wall after DVT (Figure 3.1).

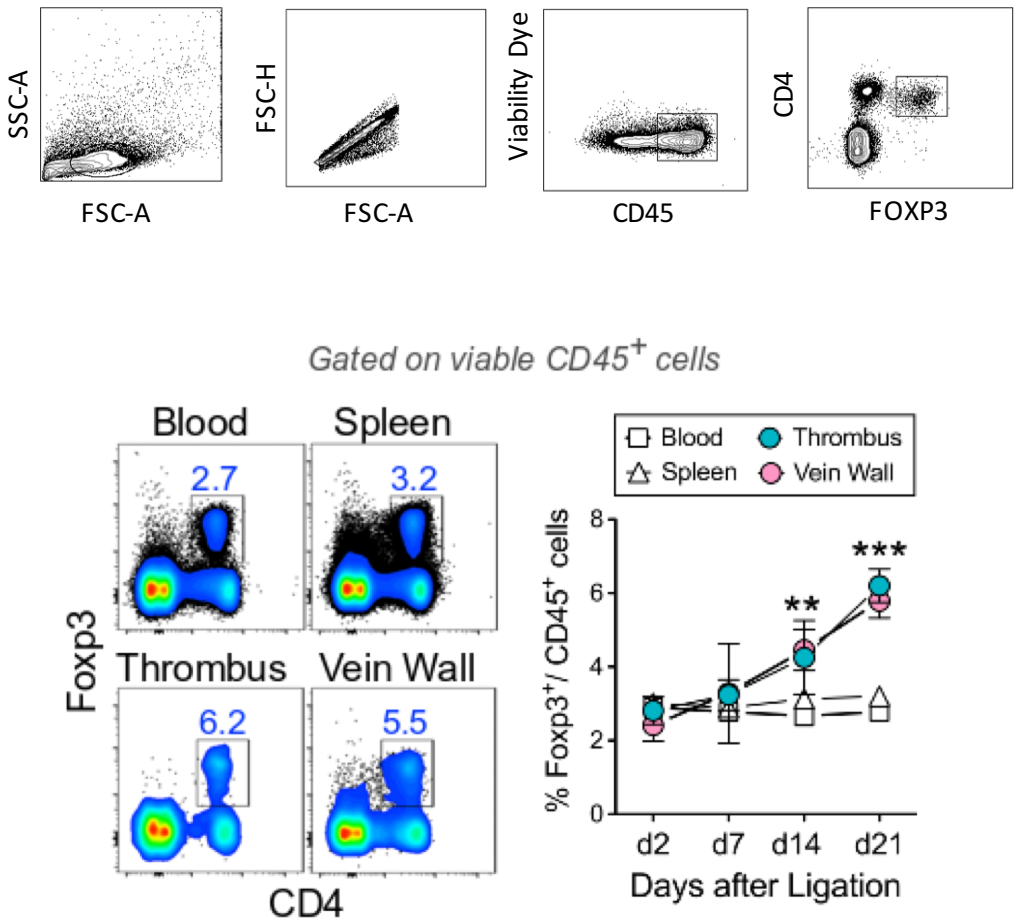


**Figure 3.1. Tregs accumulate in venous thrombi and vein walls.** (A) Gating Strategy for Treg cells. Lymphocytes are identified based on their forward and side scatter exclusion of doublets and dead cells. Finally, Foxp3+ CD4+ T cells are gated on viable CD45+ Cells. (B)

Representative flow cytometric analysis of Foxp3+ expression on CD4+ cells after DVT induction up to 21 days. Foxp3+ expression on T cells. Data show mean ± SEM, *p 0.05; **p 0.01; *** p 0.001, ns, non-significant. Data are representative of at least three independent experiments.

CD69 is an activation marker induced by either antigen or soluble factors in T cells. A subpopulation of approximately one-third of the lymphatic Tregs expresses CD69. Although both CD69+ and CD69- Tregs exist in hemostasis, CD69-expressing cells have more potent suppressor activity (Cortés et al., 2014). Further investigating the phenotype of Treg cells in thrombi and thrombotic vein walls we observed a strong up-regulation of CD69 by Tregs in the thrombus and surrounding vein wall and its expression was elevated progressively as thrombi aged, indicating local Treg cell activation upon recruitment. In contrast, DVT did not affect CD69+ Treg numbers in the blood and lymphatics (Figure 3.2).

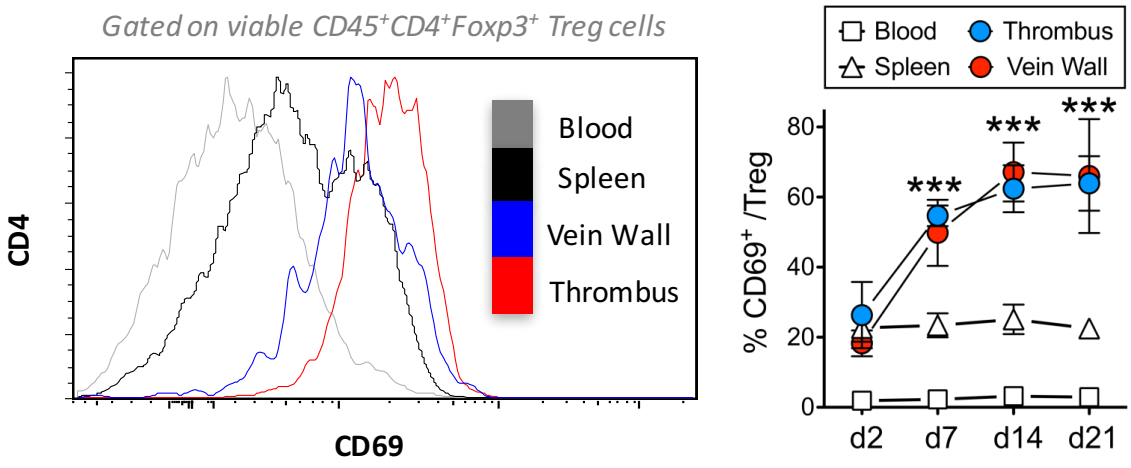


**Figure 3.2. CD69 expression on CD4+ cells.** (A) Increase of CD69+ CD4+ T cells in the vein wall and thrombus compared to the blood and spleen. (B) CD4+ Foxp3+ cells up-regulate CD69 after DVT induction for up to 21 days. Data show mean ± SEM, *p 0.05; **p 0.01; *** p 0.001, ns, non-significant. Data are representative of three independent experiments each with n = 5-8 per group.

Evaluation of additional markers revealed that Treg cells accumulating in the thrombus and vein wall after DVT gradually acquire a uniquely activated

(CD69⁺CD62L⁻) tissue-resident (KLF2$^{neg}$) Th1-Treg (CXCR3⁺ T-bet⁺) phenotype in comparison with lymphoid-organ Tregs (Figure 3.3) (Pabbisetty et al., 2016; & Tauro et al., 2013).

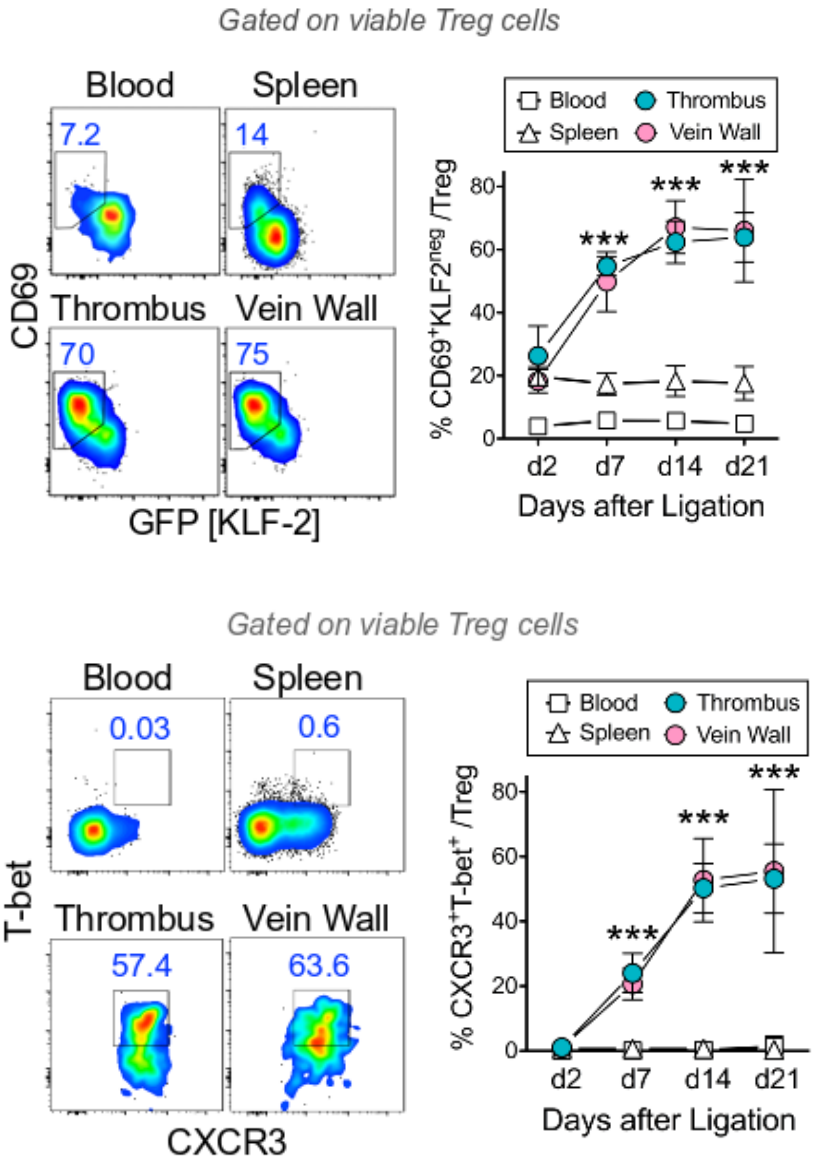


**Figure 3.3. Phenotype of CD4⁺ Foxp3⁺ CD69⁺ cells from thrombotic mice 14 days after DVT induction.** Representative flow cytometric analysis of (A) KLF2 vs CD69, (B) T-bet vs CXCR3 and cells isolated from blood, spleen and thrombotic tissues 14 days after DVT induction. (A) CD69⁺ CD4⁺ Foxp3⁺ cells down-regulate KLF2 expression after DVT induction in thrombus and vein wall. (B) Increased CXCR3⁺ CD69⁺ CD4⁺ Foxp3⁺ cell subsets in thrombotic tissues are T-bet dependent. Data show mean ± SEM, *p 0.05; **p 0.01; *** p 0.001, ns, non-significant. Data are representative of three independent experiments each with n = 4-5 per group.

### 3.2. Treg Expansion or Removal

To understand the importance of Treg cells in DVT, we set out to compare the course of thrombus formation and resolution in the absence of Tregs or in presence of increased Treg numbers. To effectively deplete Tregs in the course of DVT we employed DEREG mice expressing a simian diphtheria toxin receptor-enhanced green fluorescent protein (DTR-eGFP) fusion protein that is under the control of the endogenous forkhead box P3 (Foxp3) promoter/enhancer regions on a BAC transgene (Figure 3.4). A single DT injection depletes 80-90% of the Treg population in DEREG mice. With repeated injection on two consecutive days, almost all Tregs are removed systemically. After their removal, the Treg compartment takes about five days to replenish with newly formed cells (Lahl et al., 2007). Furthermore, cell death induced by DT administration is apoptotic and hence does not trigger a pro-inflammatory immune response.

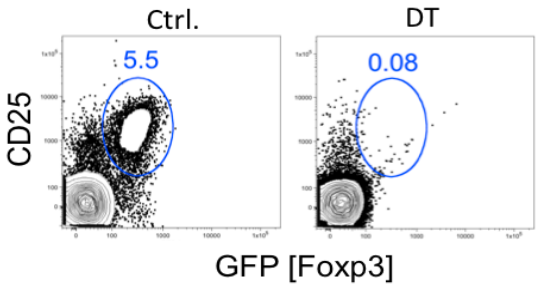


**Figure 3.4. Frequency of Foxp3+ cells for DT and control DEREG mice.** Routinely, 85-90% of Treg cells are eliminated in the spleen.

Conversely, we injected recombinant IL-2/anti-IL-2 (JES6-1) mAb complexes prior or upon DVT induction to specifically expand Treg numbers. Injection of a total dose of 6 µg (5 µg anti-IL-2 mAb (JES6-1) plus 1.5 µg mrIL-2) intraperitoneally for four consecutive days caused a rapid body-wide expansion of Treg cells with an average of a 6 to 8-fold increase in numbers compared to baseline. In accordance with previous observations (Dinh et al., 2012), IL-2 complex injection did not affect the differentiation state of Tregs in lymphatics or thrombotic veins (Figure 3.5).

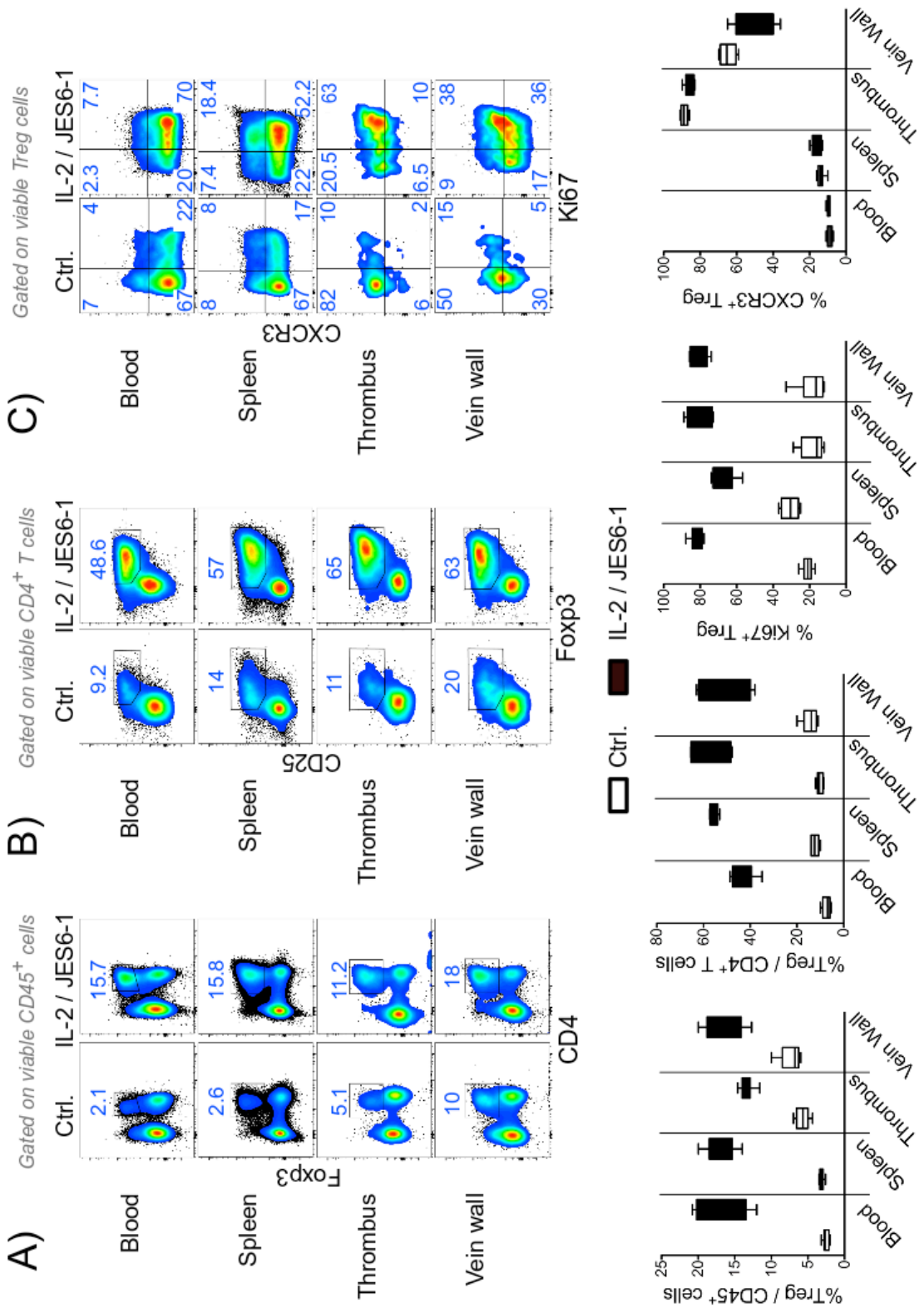


**Figure 3.5. The effect of IL-2/anti-IL-2 mAb complexes on CD4+ Foxp3+ Treg cells in DVT-induced mice.** (A and B) Representative flow cytometry plots of CD4+ Foxp3+ Treg cells frequencies in DVT-induced mice compared to control mice after IL-2/anti-IL-2 mAb treatment. (C) Representative flow cytometry plots of CXCR3 and Ki67 expression among

$CD4^+$ $Foxp3^+$ Tregs isolated from blood, spleen, and thrombotic tissues DVT-induced mice compared to control mice after IL-2/anti-IL-2 mAb treatment. (C) Expansion of Treg cells and expression of CXCR3 and Ki6 marker on expanded Treg cells in the spleen, blood, and thrombotic tissue after IL-2/anti-IL-2 mAb treatment. Data show mean ± SEM, *p 0.05; **p 0.01; *** p 0.001, ns, non-significant. Data are representative of three independent experiments each with n = 4-5 per group.

### 3.3. Treg Ablation Before DVT Induction

DT injection on two consecutive days prior to DVT induction did not affect thrombus formation but dramatically increased the inflammatory response in thrombotic veins as reflected by a persistent $Ly6C^{hi}$ monocyte phenotype in thrombi. This observation shows that Tregs dampen post-thrombotic inflammation, which corresponds to their known role in immune regulation. Since the inflammatory response did not abate in Treg-depleted animals, the experiments were stopped after seven days.

### 3.4. Treg Ablation or Expansion During Thrombus Resolution

While the effect of Treg cells in initial post-thrombotic inflammation could possibly be predicted from their known function in the immune system (Josefowicz et al., 2012), their involvement in reorganisation and resolution of venous thrombi remained uncertain. In order to identify such a possible involvement, we depleted Tregs for two consecutive days beginning at day eight and nine after DVT and followed the course of healing by high-frequency ultrasound.

Temporally-delayed Treg cell depletion significantly delayed thrombus resolution signifying a role in tissue reorganisation. Notably, an additional third Treg depletion on day 14 further slowed thrombus resolution, revealing that ordered venous thrombus resolution is dependent on Tregs. Conversely, IL-2/anti-IL-2-mediated Treg cell expansion in late-onset DVT, significantly shortened the time until thrombus resolution (Figure 3.6).

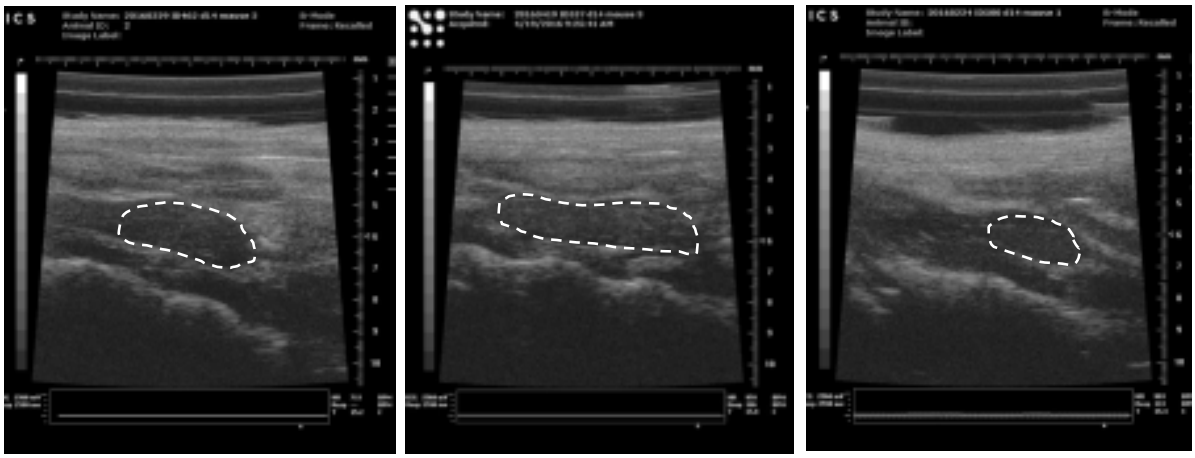

Crtl. Depl. Complexes.

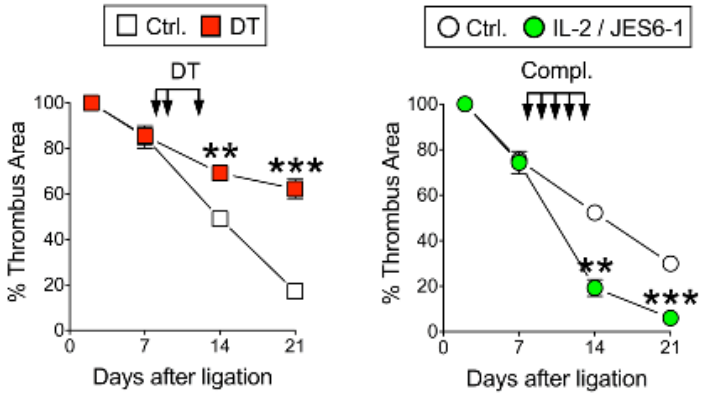


**Figure 3.6. Absence and expansion of Treg cells affects thrombus resolution/repair.** (A) Representative images obtained by high-frequency ultrasound (HFUS) of thrombi in untreated, Treg-depleted and IL-2/anti-IL-2 mAb treated B6 mice on day 14 after DVT induction. (B) Thrombus sizes determined by HFUS of thrombi in untreated, Treg-depleted and IL-2/anti-IL-2 mAb treated B6 mice at indicated time points after ligation compared with day 2. Data show mean ± SEM, *p 0.05; **p 0.01; *** p 0.001, ns, non-significant. Data are representative of three independent experiments each with n = 6-8 per group.

In order to identify changes in the composition and/or structure of thrombi induced by the absence or increased number of Treg cells, we histologically examined healing thrombi at different time points within the experimental groups (Undas et al., 2011). Histology confirmed delayed and enhanced thrombus resolution induced by Treg depletion and expansion, respectively. (Figure 3.7).

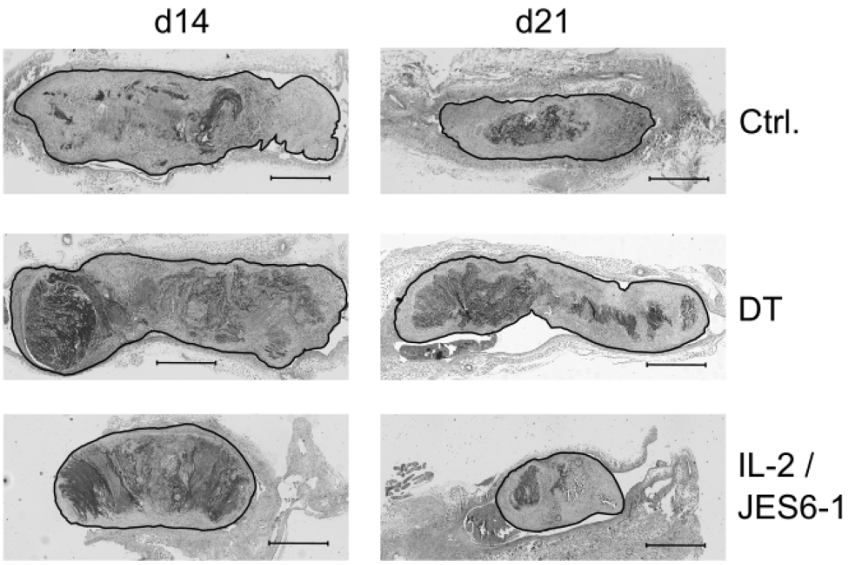


**Figure 3.7. Absence and expansion of Treg cells affects thrombus size.** Representative images after Carstairs staining of IVC in untreated, depleted and IL-2/anti-IL-2 mAb treated mice after 14 and 21 days. Magnification ×200 µm, objective 10X. (Stitched 6-8 pictures). Data are representative of three independent experiments each with n = 4-7 per group.

### 3.5. Treg Ablation or Expansion Affects Thrombus Composition

In addition to size differences, Treg manipulation altered numerous histological features. These differences were particularly evident in the Carstairs staining that distinguishes fibrin (red), collagen (blue) and erythrocytes (orange) (Gu et al, 2011). Compared to untreated controls, thrombi in Treg-depleted animals contained less collagen, and the collagen area was further increased upon Treg expansion, indicating increased fibrin degradation and collagen build-up in the presence of Tregs (Figure 3.8-10). A further difference was in vein wall thickness: While in the control group and complex-treated mice, the thickness of the venous wall increased throughout thrombus resolution, depleted animals showed a smaller change. In accordance with the notion of monocyte-mediated collagen build-up, thrombi of Treg-depleted mice contained fewer monocytes/macrophages (Figure 3.8 and 3.9) (Liu Cassado., 2017). Neovascularisation, as a critical event in the process of thrombus resolution was detected by CD31 staining (Liu et al, 2012). In the sections endothelial cells appear as a thin layer of cells lining the luminal surface of the vessel wall. The vessel-rich area and vessel density significantly increased in the Treg-depleted group

on days 14 and 21 and decreased upon Treg expansion (Figure 3.8 and 3.9), revealing increased neovascular channel formation in the absence of Tregs.

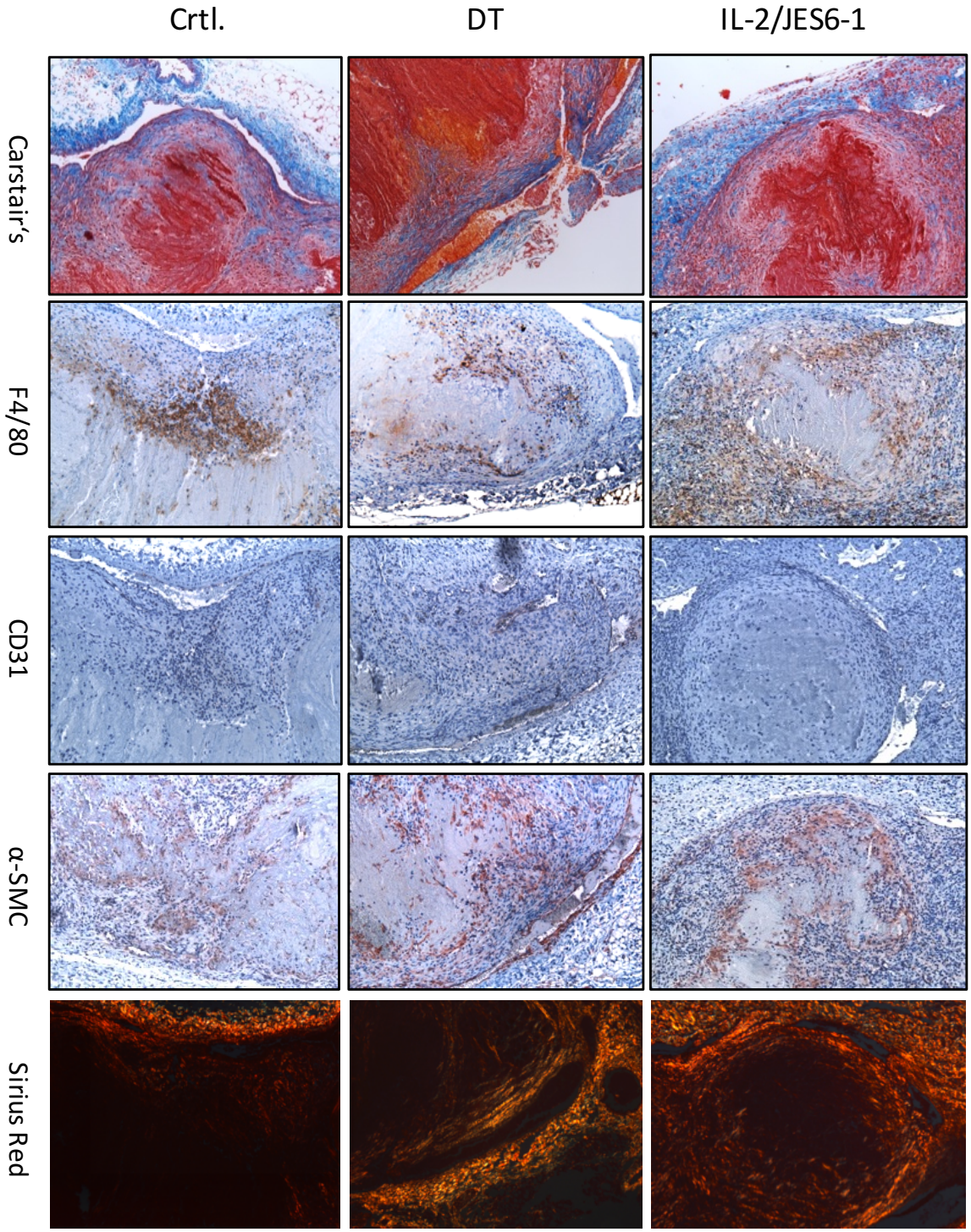


**Figure 3.8. Absence and expansion of Treg cells affects the thrombus maturity and resolution morphological characteristics on day 14 after DVT.** (A) Representative images after Carstair's (thrombus organisation), F4/80 (Macrophages), CD31 (endothelial cells), α-SMA (myofibroblasts) and sirius red (interstitial collagens) staining of IVC section in untreated, depleted, and IL-2/anti-IL-2 mAb treated mice. Magnification ×50 µm, objective 20X. Data are representative of three independent experiments each with n = 4-7 per group.

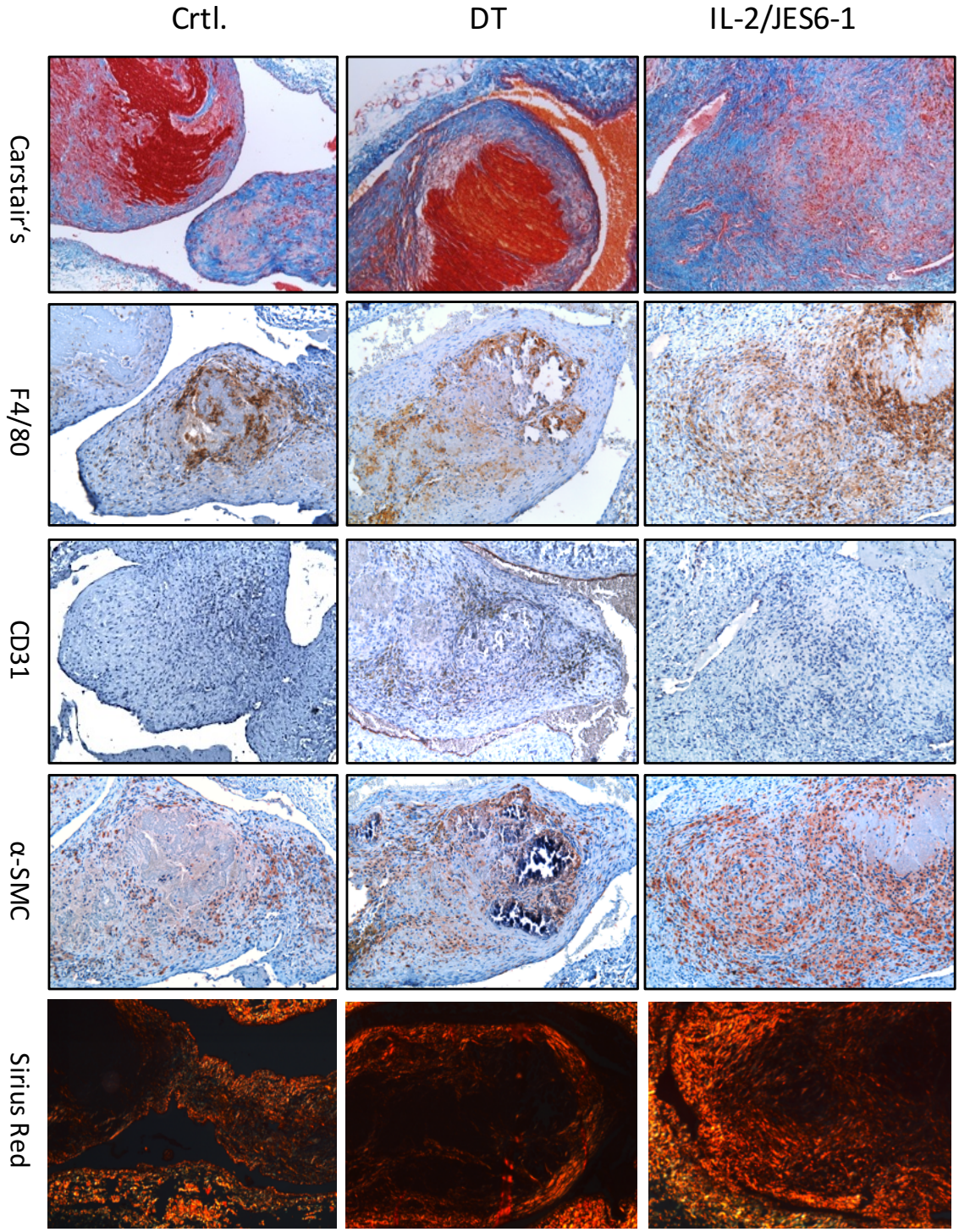


**Figure 3.9. Absence and expansion of Treg cells affects the thrombus maturity and resolution morphological characteristics on day 21 after DVT.** (A) Representative images after Carstair's (thrombus organisation), F4/80 (Macrophages), CD31 (endothelial cells), α-SMA (myofibroblasts) and sirius red (interstitial collagens) staining of IVC section in untreated, depleted, and IL-2/anti-IL-2 mAb treated mice. Magnification ×50 µm, objective 20X. Data are representative of three independent experiments each with n = 4-7 per group.

We also looked at myofibroblast activation by carrying out α-SMC staining. α-SMC is, an isoform typical of contractile smooth muscle cells and a good marker for VSMC (Rzucidlo et al, 2007). In the depleted group, we only saw α-SMA expression around the fibrin area whereas Treg cell expansion increased myofibroblast activation all over thrombus area in a highly-organised region most significantly at day 14 (Figure 3.8, 3.9, 3.10). The latter results demonstrate increased EndMT transition in the presence of increased Treg numbers.

Sirius red staining is one of the most important stains used to study collagen networks and tissue remodelling in various tissues due to its specific reactivity to most collagen types. In polarised light, the thickest collagen fibres appear red while the finest appear yellow (newly formed threads) and are easily differentiated from the black background, hence allowing for quantitative estimations of tissue fibrosis (Vogel et al, 2015). While Treg depletion reduced the formation of new fibres, Treg expansion increased collagen accumulation and thrombus maturation confirming results of Carstairs staining (Figure 3.8 and 3.9).

### 3.6. Tregs Instruct Myeloid Cell Differentiation in Resolving Thrombi

Inflammatory and patrolling monocytes play differential roles in venous thrombus formation and resolution by virtue of different coagulant, inflammatory and fibrinolytic activities. Conversion of procoagulant, inflammatory Ly6C$^{hi}$ monocytes to reparative and pro-angiogenic Ly6C$^{neg}$ monocytes and subsequent further differentiation into macrophages and dendritic cells appears to be important in thrombus re-organisation and resolution. We therefore further analysed the composition and enzymatic activity of monocyte populations in resolving thrombi by flow cytometry in Treg-manipulated and control mice.

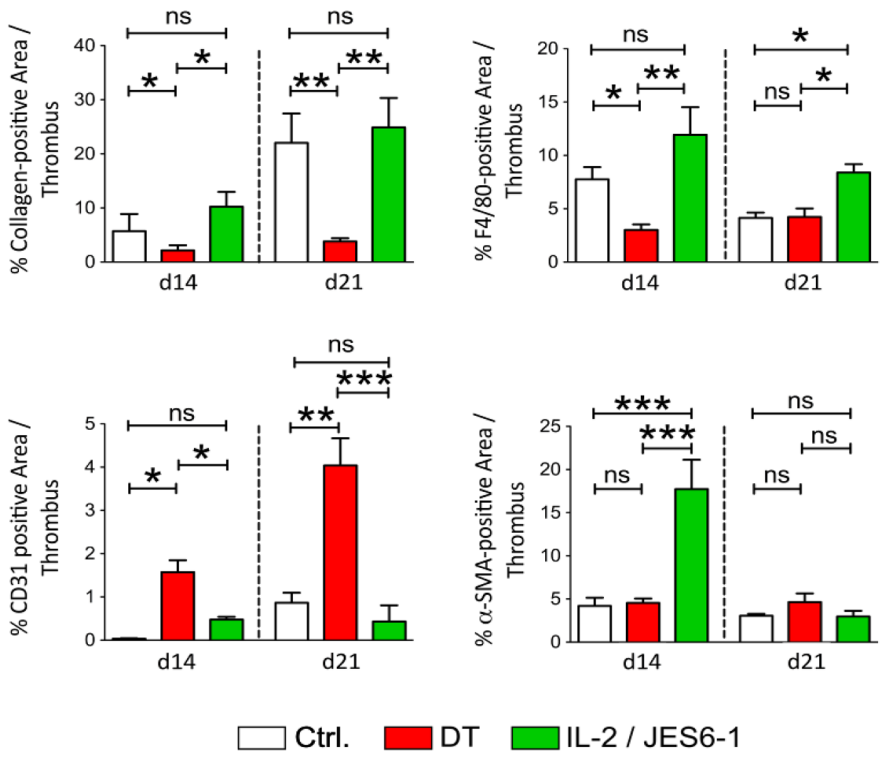


**Figure 3.10. Collagen formation, macrophage present, micro vessel density and myofibroblast activation in untreated, depleted, and IL-2/anti-IL-2 mAb treated mice.** Summary of the quantitative analysis, mean areas of immunohistochemical staining in the thrombus area 14 and 21 days after DVT induction. Data show mean ± SEM, *p 0.05; **p 0.01; *** p 0.001, ns, non-significant. Data are representative of three independent experiments each with n = 4-7 per group.

The monocyte switched from a pro-inflammatory, Ly6C$^{hi}$ to a primarily anti-inflammatory, Ly6C$^{int/lo}$. This was enhanced in complex-treated mice compared to controls and significantly retarded in Treg-depleted mice (Figure 3.11). While a certain population of CD45$^{+}$ Lin$^{-}$ CD11b$^{+}$ CD115$^{+}$ Ly6C$^{int}$ reparatory monocytes showed MMP activity at day 14 after DVT in complex-treated mice, fewer such cells could be observed in controls and MMP activity was minimal in Treg-depleted thrombi (Figure 3.11). CD11b$^{+}$ DCs populations can be distinguished according to surface phenotype, monocyte-derived DCs with CD45$^{+}$ Lin$^{-}$ CD11c$^{+}$ CD11b$^{hi}$ MHC-II$^{+}$ expression profile and the migratory DCs with CD45$^{+}$ Lin$^{-}$ CD11c$^{+}$ CD11b$^{hi}$ MHC-II$^{-}$ (Qu et al, 2014; & Domínguez et al, 2010).

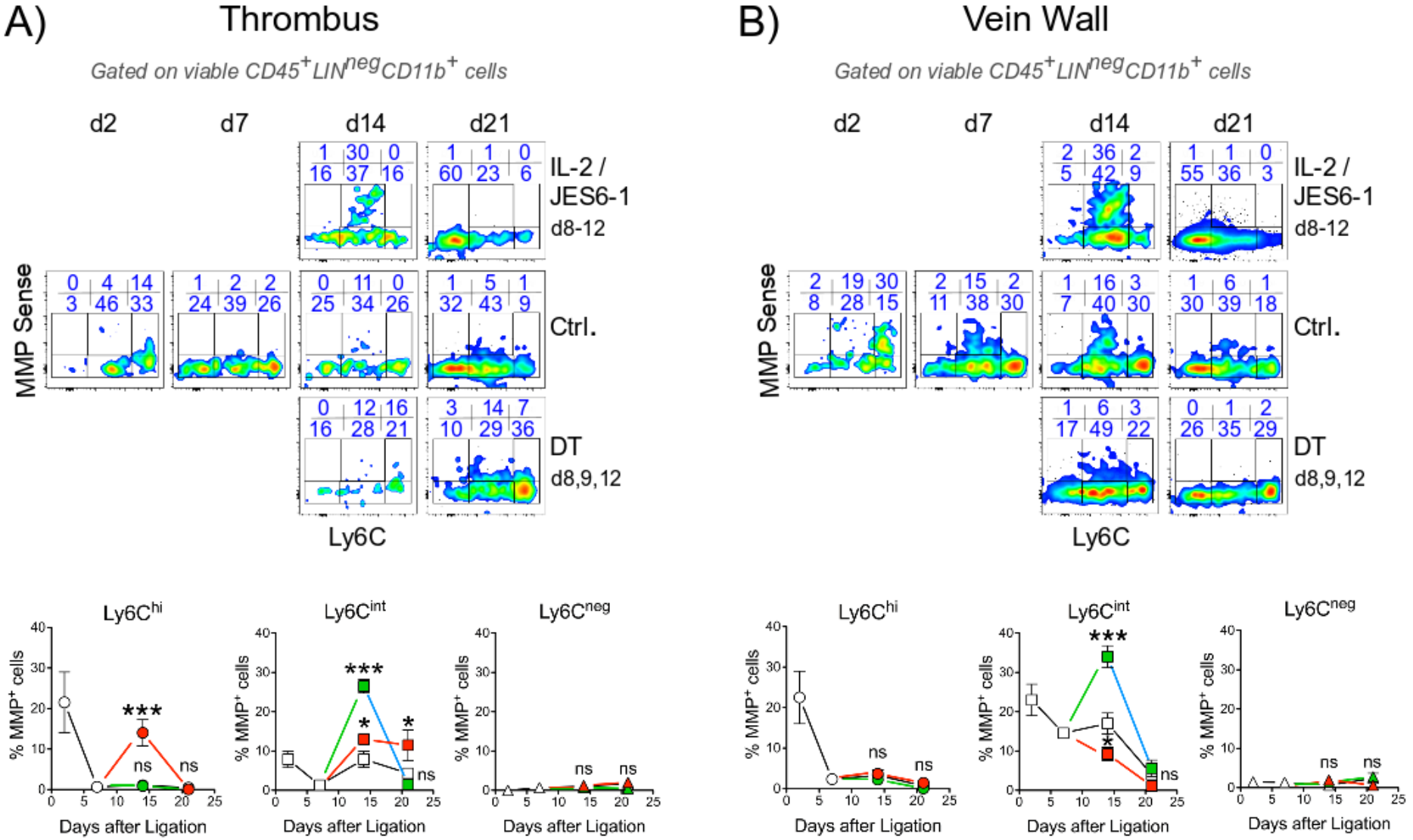
A)
Thrombus
Gated on viable CD45+LINnegCD11b+ cells
d2
d7
d14
d21
IL-2 / JES6-1 d8-12
Ctrl.
DT d8,9,12
MMP Sense
Ly6C
Ly6Chi
Ly6Cint
Ly6Cneg
% MMP+ cells
Days after Ligation
B)
Vein Wall
Gated on viable CD45+LINnegCD11b+ cells
d2
d7
d14
d21
IL-2 / JES6-1 d8-12
Ctrl.
DT d8,9,12
MMP Sense
Ly6C
Ly6Chi
Ly6Cint
Ly6Cneg
% MMP+ cells
Days after Ligation

**Figure 3.11. Treg influence monocyte population by MMP production after DVT induction in untreated, depleted and IL-2/anti-IL-2 mAb treated mice up to 21 days.** (A) Identification of MMP sense-positive monocytes 24 after injection by flow cytometry 2, 7, 14, and 21 days after DVT in thrombus (A) and vein wall (B). Flow cytometry plot of $CD45^{+}$ $Lin^{-}$ $CD11b^{+}$ $CD115^{+}$ cells are gated on viable cells. (A and B Below) Summary of the flow cytometry analysis. The frequency of $MMP^{+}$ cells among $Ly6C^{hi}$, $Ly6C^{int}$, and $Ly6C^{neg}$ monocyte. Data show mean ± SEM, *p 0.05; **p 0.01; *** p 0.001, ns, non-significant. Data are representative of three independent experiments each with n = 3-4 per group.

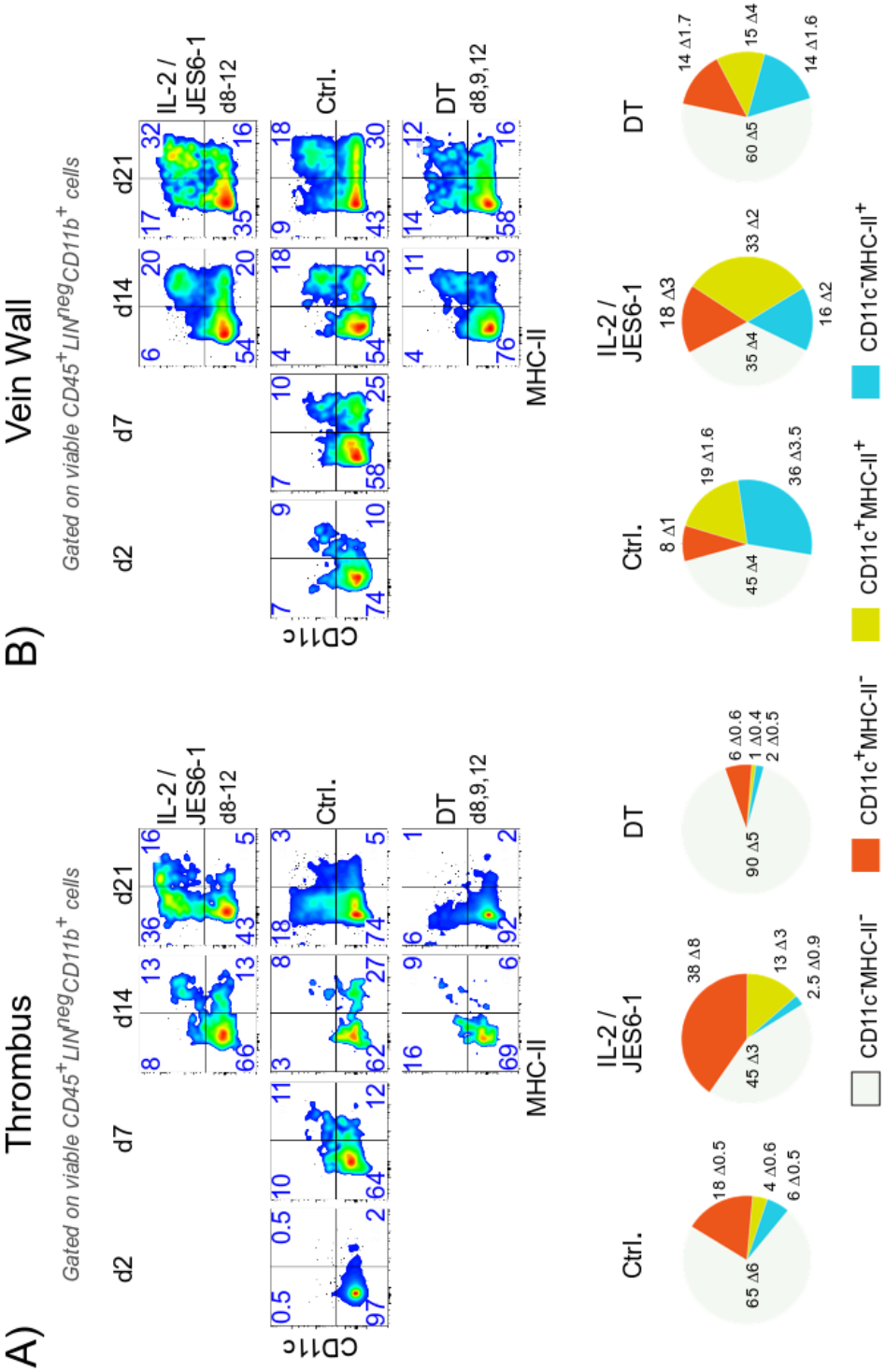

**Figure 3.12. Tregs influence monocyte differentiation after DVT in untreated, depleted and IL-2/anti-IL-2 mAb treated mice overtime.** (A) Heterogeneous CD $11^{+}$ DC derive from monocytes in the thrombus (A) and vein wall (B). Flow cytometry plot of $CD45^{+}$ $Lin^{-}$ $CD11b^{+}$ cells are gated on viable cells. (A and B below) Summary of the flow cytometry analysis. The frequency of $MMP^{+}$ cells among $Ly6C^{hi}$, $Ly6C^{int}$, and $Ly6C^{neg}$ monocyte. Data show mean ± SEM, *p 0.05; **p 0.01; *** p 0.001, ns, non-significant. Data are representative of three independent experiments each with n = 3-4 per group.

Whereas DCs only formed a small population in the thrombi of control mice a significantly abundant population was detected in the thrombi of complex treated mice, and appeared to accumulate over time (Figure 3.12). These results show that Tregs significantly influence the development of monocytes recruited into thrombi, including enzymatic activity required in tissue reorganisation. In addition to the thrombus, we also examined the adjacent venous wall. The changes of the monocytes described for the thrombus also take place in the vein wall, but appear to be different compared to in the thrombus.

### 3.7. Thrombus Tregs Express a Repair Treg Profile

In addition to their phenotyping along known differentiation markers, we investigated the expression profile of Tregs in healing thrombi using RNA-Seq. For this purpose, $CD45^+$ $CD4^+$ GFP $(Foxp3)^+$ $CD69^+$ Tregs were FACS-sorted from day 14 thrombi and spleens of ligated DEREG mice (Figure 3.13).

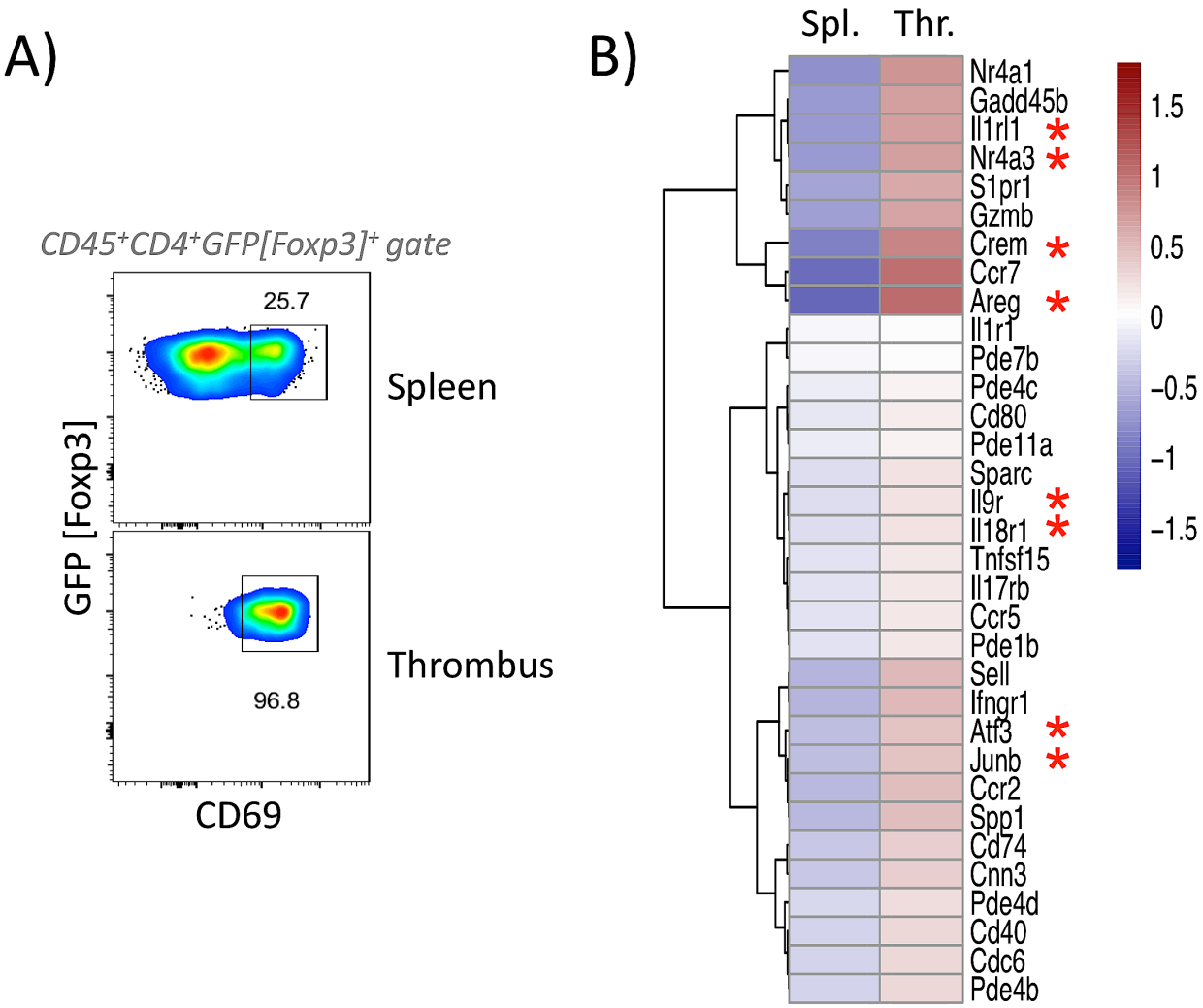


**Figure 3.13. CD69 Treg cells display a distinct gene expression profile.** (A) $CD45^+$ $CD4^+$ GFP $(Foxp3)^+$ $CD69^+$ Treg were FACS-sorted on day 14 thrombi and spleens of ligated DEREG mice. (B) Heatmap of genes with significant gene expression with FACS-sorted Treg cells. (Pictures kindly provided by Federico Marini).

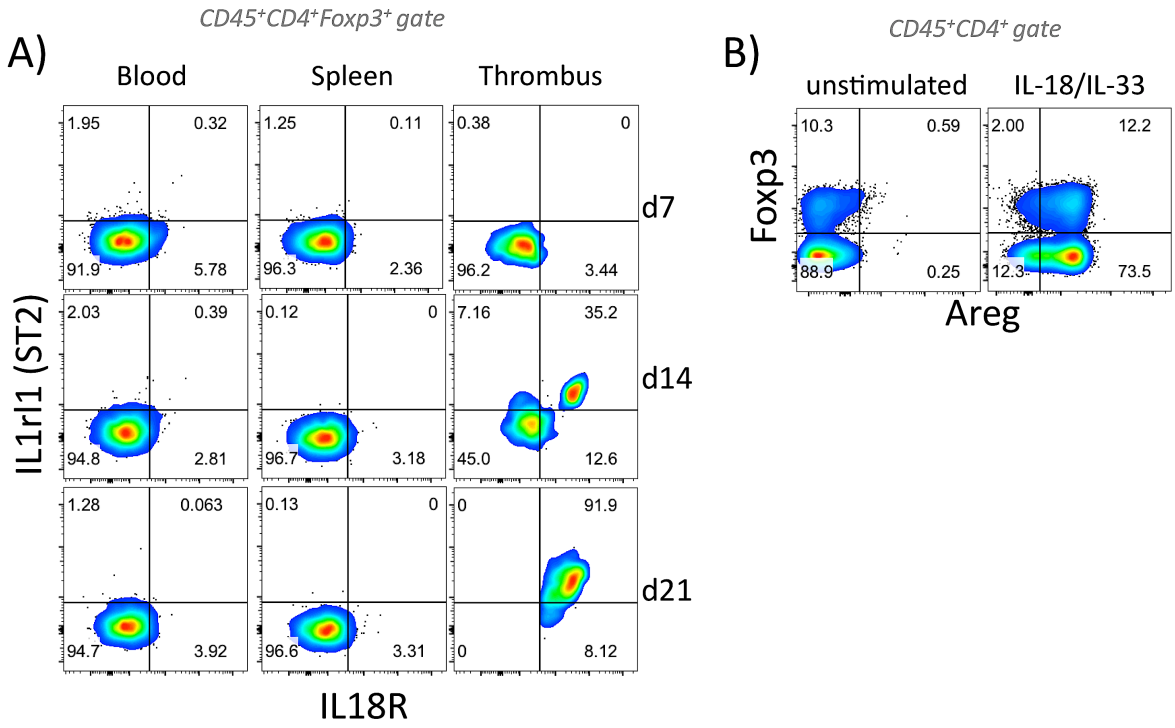


**Figure 3.14. IL-18R and IL1rl1 (ST2) expression and amphiregulin production by Treg cells. (**A) Representative flow cytometry plots depicting ST2 and or IL-18R expression determined by flow cytometric analysis of CD4+ Foxp3+ Treg cells isolated from blood, spleen and thrombus of C57BL/6 mice on days 7, 14, and 21 after DVT induction . (B) Representative flow cytometry plots showing amphiregulin production of CD4+ Foxp3+ Treg cells from DEREG mice in the presence of IL-18, and IL-33, or without stimulation after 4 hours in vitro.

Comparison of the expression profiles of sorted populations and subsequent confirmation of selected markers by flow cytometry revealed a 'repair Treg signature' of thrombus-resolving Tregs similar to the one previously described in injured muscles Tregs. This profile is characterised by the expression of the IL-33 receptor (ST2), the IL-18 receptor and the formation of amphiregulin (Figure 3.14). In addition, we were also able to identify molecules, not previously described for Tregs, that require further analysis with respect to their role in thrombus resolution and, particularly, monocyte differentiation (Figure 3.13).

## 4. DISCUSSION

I was able to show herein that Treg cells accumulate upon DVT in the thrombus and vein wall, become activated and differentiate into tissue-resident Th1 repair Tregs. Punctual, selective, Treg depletion or expansion during thrombus resolution dramatically impairs or enhances thrombolysis respectively. Treg-dependent acceleration and delay of thrombus resolution is accompanied by marked phenotypic and functional changes of the myeloid compartment. ‘thrombus-busting’ Treg cells thus appear to be required in ordered thrombus resolution and supposedly regulate matrix remodelling by controlling monocyte infiltration/differentiation.

Treg cells are rapidly recruited into inflamed tissue where they attenuate inflammatory responses. Their ability to enter inflamed tissue is due to the expression of receptors for inflammatory chemokines (Gratz et al., 2014; Campbell et al., 2015; & Huehn et al., 2004).

These include receptors that lead cells to Th1, Th2 or Th17 mediated inflammatory reactions, such as CXCR3, CCR8 and CCR6, and more general inflammatory receptors such as CCR2 and CCR5. In the absence of these receptors, recruitment and anti-inflammatory effects of Tregs are impaired (Hirota et al., 2007; & Zhang et al., 2009). In addition, Treg cells express integrins such as αLβ2-Integrin (LFA-1) and α4β1-Integrin (VLA-4), which increase their migration into inflamed tissue (Glatigny et al., 2015).

In a previous study, we were able to show that post-thrombotic inflammation is a Th1 reaction involving interferon gamma-forming T cells (Luther et al., 2016). We therefore assume that Tregs, which migrate into the thrombus, have the ability to react to the inflammatory reaction in this tissue. Small populations of CXCR3-expressing Tregs exist in the spleen and blood, and should be capable of doing so. However, further investigations on Treg-specific CXCR3-deficient animals would be necessary to verify this assumption.

Treg cells can be divided into $CD44^{lo}$ $CD62L^{+}$ 'central' Treg cells and $CD44^{hi}$ $CD62L^{lo/neg}$ 'effector' Treg cells by differential expression of the activation marker CD44 and the lymph node homing receptor CD62L (Smigiel et al., 2014). While 'central' Treg cells show little dividing activity and circulate through secondary lymphatic tissue,

'effector' Treg cells are highly proliferative and form the dominant Treg cell population in non-lymphoid tissues.

Thus, there would be two populations specialised to function either within the secondary lymphoid tissue or in certain non-lymphoid tissues (Cretney et al., 2013). Since the Tregs we found in thrombi, are uniformly negative for CD62L, unlike those found in the spleen, we can assume that they belong to or originate from the second population.

With regards to their formation, thrombus Tregs appear to most likely be thymus-derived. This is supported by the inflammatory reaction in the thrombus which does not correspond to the conditions of pTreg development from naive $CD4^+$ T cells, and we have also found that Tregs express Helios uniformly in thrombi. Even if Helios alone cannot unequivocally prove thymic origin (Szurek et al., 2015), it does at least support their effector cell status (Akimova et al., 2011) which, in turn, supports the assumption of thymic rather than peripheral development.

The activation modalities of Treg cells, especially whether they react against self-antigens, are controversially discussed (Jordan et al., 2001; Apostolou et al., 2002; Sprouse et al., 2018; & van Santen et al., 2004). Tregs in thrombi are characterised by expression of C-type lectin CD69 and decreased expression of zinc finger transcription factor KLF2 (Carlson et al., 2006), which, by reducing L-selectin (CD62L) and phospholipid sphingosine-1-phosphate receptor (S1P1R) expression, are known to prevent cells in tissues returning to lymphatic organs (Skon et al., 2013; & Shiow et al., 2006).

In addition to defining a tissue resident state, CD69 is also an activation marker and although $CD69^+$ and $CD69^-$ $FoxP3^+$ Tregs are present in homeostasis, only $CD69^-$ expressing Tregs express high levels of CTLA-4, ICOS, CD38 and GITR suppression-associated markers, secrete high amounts of TGFβ and have a strong suppressor activity. CD69 expression can be induced both by activation via T cell receptors and by cytokines such as TNF-α, type I interferons and IL-33 alone (Kohlmeier et al., 2010; & Skon et al., 2013).

Comparative in vitro studies have also shown that CD69 expression on Tregs can be particularly easily altered by cytokines (Bremser et al., 2015). Meanwhile, ‘repair’ Tregs have been shown to be activated by inflammatory cytokines rather than antigen in non-lymphatic tissues (Arpaia et al., 2015). Given the inflammatory milieu

in thrombi and the absence of clearly defined vascular T cell antigens, antigen-independent activation of Treg in thrombi appears likely.

Because thrombi are continuously degraded in healthy individuals over time, recruited Treg cells cannot remain permanently in this tissue. However, our data show that they stay in this tissue for at least the entire period of thrombus resolution. What happens to them afterwards, whether they return to the lymphatic tissues or die, is unclear. It is currently assumed that the inflammation-experienced Treg cell population loses its activation-induced changes and its enhanced suppressive function once inflammation has calmed down (van der Veeken et al., 2016). It is speculated that this loss of memory may help to avoid generalised immunosuppression that could otherwise result from repeated activation of accumulating memory Tregs.

The function of Treg cells has been attributed to a growing number of different pathways, molecules and processes. This has led to conflicting conclusions and the interim assumption that Tregs are allegedly 'a jack of all trades' (Tang et al., 2008). In fact, countless mechanisms have been proposed without checking pre-existing mechanisms, so that it remains largely unclear which mechanisms actually exist and in which populations. Tregs in non-lymphoid tissues have only been studied for a few years. The best characterised tissue Treg populations are those in VAT (Feuerer et al., 2009; & et al., Burzyn 2013) and colon lamina propria (Cebula et al., 2013; Geuking et al., 2011; & Atarashi et al., 2011).

Tissue Tregs appear to have a variety of origins, depending on the particular tissue examined. However, they appear to be already fully differentiated when they enter the particular tissue. Determining where and when tissue Tregs adopt their characteristic phenotypes requires well designed line tracking experiments using either inducible fluorescence reporter lines or transgenic tissue Tregs.

In all tissue Tregs, IL-33 appears to be a critical factor for local proliferation and stability. In contrast, this cytokine has a significantly lower effect on classical lymphoid Treg populations reflecting their low expression of the IL-33 (ST2) receptor. The differential dependence on IL-33 (Schiering et al., 2014) also seems to make sense, considering the alarm function of IL-33 and the potent tissue repair programs by this factor (Molofsky et al., 2015). Based on this commonality, tissue Tregs appear to express IL-33-dependent molecules such as tissue-repair factor amphiregulin

(AREG) and KLRG-1. Consistent with their local role in thrombus resolution, we find KLRG-1 and ST2 expressed in thrombus Tregs.

Certainly, some of the activities of tissue Tregs are directed at controlling inflammatory cells in the vicinity. Monocytes have an important role in peripheral T cell polarisation, reside in close proximity to repair Tregs in injured tissues and are the main source of factors that drive local repair of Tregs. Their local differentiation from pro- to anti-inflammatory activity is required for effective tissue repair (Wynn et al., 2016).

Their programming by tissue Tregs seems particularly obvious since it coincides with new ideas on the establishment of tissue-specific macrophage phenotypes (Lavin et al., 2014; & Gosselin et al., 2014). For thrombus Treg cells it could be shown in this work that they enhance the differentiation of myeloid cells into DCs. However, it is still unclear which functional consequences this programming direction has on thrombus resolution.

For immunologists, tissue Tregs are an important new cell population whose properties need to be further investigated. In this context, some questions appear to be of particular importance: How are Tregs attracted and preserved by certain tissues? What is the distinction between different tissue Tregs? What processes do tissue Tregs target within certain tissues? Can the function of tissue Tregs be replaced by recombinant factors? With regard to thrombus Treg, the investigation of these issues has only just begun.

## 5. CONCLUSION

In this study it was shown for the first time that Treg cells migrate into venous thrombi, become activated and influence the course of thrombus resolution by regulating the differentiation of infiltrating monocytes. Further functional studies will be necessary to find out how they actually control monocyte differentiation in thrombi. It is, however, already clear, that thrombus Tregs may provide new therapeutic opportunities for DVT patients. Analogous to the procedure in mice, Treg cells can be expanded in humans by low-dose IL-2. Motivated by the findings in this work, pilot experiments will soon begin within the framework of studies to find out whether DVT patients can benefit from Treg cell expansion.

## 6. REFERENCES


Aghourian, M.N., Lemarié, C.A., & Blostein, M.D. (2012) In vivo monitoring of venous thrombosis in mice. J Thromb Haemost. 10, 447-52. doi: 10.1111/j 1538-7836.2011. 04615.x.

Akimova, T., Beier, U.H., Wang, L., Levine, M.H., & Hancock, W.W. (2011) Helios expression is a marker of T cell activation and proliferation. PLoS One. 6, e24226. doi: 10.1371/journal.pone.0024226.

Apostolou, I., Sarukhan, A., Klein, L., & von Boehmer H. (2002) Origin of regulatory T cells with known specificity for antigen. Nat Immunol. 3, 756-63. doi: 10.1038/ni816.

Arpaia, N., Green, J.A., Moltedo, B., Arvey, A., Hemmers, S., Yuan, S., Treuting, P.M., & Rudensky, A.Y. (2015) A distinct function of regulatory T cells in tissue protection. Cell. 62, 1078-89. doi: 10.1016/j.cell.2015.08.021.

Atarashi, K., Tanoue, T., Shima, T., Imaoka, A., Kuwahara, T., Momose, Y., Cheng, G., Yamasaki, S., Saito, T., Ohba, Y., Taniguchi, T., Takeda, K., Hori, S., Ivanov, I.I., Umesaki, Y., Itoh, K., & Honda, K. (2011) Induction of colonic regulatory T cells by indigenous Clostridium species. Science. 331, 337-41. doi: 10.1126/science.1198469.

Baldwin, J.F., Sood, V., Elfline, M.A., Luke, C.E., Dewyer, N.A., Diaz, J.A., Myers, D.D., Wakefield, T., & Henke, P.K. (2012) The role of urokinase plasminogen activator and plasmin activator inhibitor-1 on vein wall remodelling in experimental deep vein thrombosis. J Vasc Surg. 56, 1089-97. doi: 10.1016/j.jvs.2012.02.054.

Beaudeux, J.L., Giral, P., Bruckert, E., Foglietti, M.J., & Chapman, M.J. (2004) Matrix metalloproteinases, inflammation and atherosclerosis: therapeutic perspectives. Clin Chem Lab Med. 42, 121-31. doi: 10.1515/CCLM.2004.024.

Bochenek, ML., Rosinus, NS., Lankeit, M., Hobohm, L., Bremmer, F., Schütz, E., Münzel, T., Konstantinides, S.,& Schäfer, K. (2017) From thrombosis to fibrosis in chronic thromboembolic pulmonary hypertension. Thromb Haemost. 117, 769-83. doi: 10.1160/ TH16-10-0790.

Boyman, O., Kovar, M., Rubinstein, M.P., Surh, C.D., & Sprent, J. (2006) Selective stimulation of T cell subsets with antibody-cytokine immune complexes. Science. 311, 1924-7. doi: 10.1126/science.1122927.

Branchford, B.R., & Carpenter, S.L. (2018) The role of inflammation in venous thromboembolism. Front Pediatr. 6, 142. doi: 10.3389/fped.2018.00142.

Brandt, M., Schönfelder, T., Schwenk, M., Becker, C., Jäckel, S., Reinhardt, C., Stark, K., Massberg, S., Münzel, T., von Brühl, M.L., & Wenzel P. (2012) Deep vein thrombus formation induced by flow reduction in mice is determined by venous side branches. Clin Hemorheol Microcirc. 56, 145-52. doi: 10.3233/CH-131680.

Bremser, A., Brack, M., & Izcue, A. (2015) Higher sensitivity of Foxp3+ Treg compared to Foxp3- conventional T cells to TCR-independent signals for CD69 induction. PLoS One. 10, e0137393. doi: 10.1371/journal.pone.0137393.

Burzyn, D., Benoist, C., & Mathis, D. (2013) Regulatory T cells in non-lymphoid tissues. Nat Immunol. 14, 1007-13. doi: 10.1038/ni.2683.

Burzyn, D., Kuswanto, W., Kolodin, D., Shadrach, J.L., Cerletti, M., Jang, Y., Sefik, E., Tan, T.G., Wagers, A.J., Benoist, C., & Mathis, D. (2013) A special population of regulatory T cells potentiates muscle repair. Cell. 155, 1282-95. doi: 10.1016/j.cell.2013.10.054.

Caley, M.P., Martins, V.L., & O'Toole, E.A. (2015) Metalloproteinases and Wound Healing. Adv Wound Care. 4, 225-34. doi: 10.1089/wound.2014.0581.

Campbell, D.J. (2015) Control of Regulatory T Cell Migration, Function, and Homeostasis. J Immunol. 195, 2507-13. doi: 10.4049/jimmunol.1500801.

Campbell, D.J., & Koch, M.A. (2011) Phenotypical and functional specialisation of FOXP3+ regulatory T cells. Nat Rev Immunol. 11, 119-30. doi: 10.1038/nri2916.

Carlson, C.M., Endrizzi, B.T., Wu, J., Ding, X., Weinreich, M.A., Walsh, E.R., Wani, M.A., Lingrel, J.B., Hogquist, K.A., & Jameson, S.C. (2006) Kruppel-like factor 2 regulates thymocyte and T-cell migration. Nature. 442, 299-302. doi: 10.1038/nature04882.

Cebula, A., Seweryn, M., Rempala, G.A., Pabla, S.S., McIndoe, R.A., Denning, T.L., Bry, L., Kraj, P., Kisielow, P., & Ignatowicz, L. (2013) Thymus-derived regulatory T cells contribute to tolerance to commensal microbiota. 497, 258-62. doi: 10.1038/nature12079.

Cheng, G., Yu, A., Dee, M.J., & Malek, T.R. (2013) IL-2R signaling is essential for functional maturation of regulatory T cells during thymic development. J Immunol. 190, 1567-75. doi: 10.4049/jimmunol.1201218.

Cipolletta, D., Feuerer, M., Li, A., Kamei, N., Lee, J., Shoelson, S.E., Benoist, C., & Mathis D. (2012) PPAR-γ is a major driver of the accumulation and phenotype of adipose tissue Treg cells. Nature. 486, 549-53. doi: 10.1038/nature11132.

Cortés, J.R., Sánchez-Díaz, R., Bovolenta, E.R., Barreiro, O., Lasarte, S., Matesanz-Marín, A., Toribio, M.L., Sánchez-Madrid, F., & Martín, P. (2014) Maintenance of immune tolerance by Foxp3+ regulatory T cells requires CD69 expression. J Autoimmun. 55, 51-62. doi: 10.1016/j.jaut.2014.05.007.

Cretney, E., Kallies, A., & Nutt, S.L. (2013) Differentiation and function of Foxp3(+) effector regulatory T cells. Trends Immunol. 34, 74-80. doi: 10.1016/j.it.2012.11.002.

De Caterina, R., D'Ugo, E., & Libby, P. (2016) Inflammation and thrombosis - testing the hypothesis with anti-inflammatory drug trials. Thromb Haemost. 116,1012-21. doi: 10.1160/TH16-03-0246.

Deatrick, K.B., Eliason, J.L., Lynch, E.M., Moore, A.J., Dewyer, N.A., Varma, M.R., Pearce, C.G., Upchurch, G.R., Wakefield, T.W., & Henke, P.K. (2005) Vein wall remodeling after deep vein thrombosis involves matrix metalloproteinases and late fibrosis in a mouse model. J Vasc Surg. 42, 140-8. doi: 10.1016/j.jvs.2005.04.014.

Deatrick, K.B., Luke, C.E., Elfline, M.A., Sood, V., Baldwin, J., Upchurch, G.R., Jaffer, F.A., Wakefield, T.W., & Henke, P.K. (2013) The effect of matrix metalloproteinase 2 and matrix metalloproteinase 2/9 deletion in experimental post-thrombotic vein wall remodeling. J Vasc Surg. 58, 1375-84. doi: 10.1016/j.jvs.2012.11.088.

Dhamne, C., Chung, Y., Alousi, A.M., Cooper, L.J., & Tran, D.Q. (2013) Peripheral and thymic foxp3(+) regulatory T cells in search of origin, distinction, and function. Front Immunol. 4, 253. doi: 10.3389/fimmu.2013.00253.

Di Nisio, M., van Es, N., & Büller, HR. (2016) Deep vein thrombosis and pulmonary embolism. Lancet. 17, 3060-73. doi: 10.1016/S0140-6736(16)30514-1.

Diaz, J.A., Hawley, A.E., Alvarado, C.M., Berguer, A.M., Baker, N.K., Wrobleski, S.K., Wakefield, T.W., Lucchesi, B.R., & Myers, D.D. (2012) Thrombogenesis with continuous blood flow in the inferior vena cava. A novel mouse model. Thromb Haemost. 104, 366-735. doi: 10.1160/TH09-09-0672.

Diaz, J.A., Obi, A.T., Myers, D.D., Wrobleski, S.K., Henke, P.K., Mackman, N., & Wakefield, T.W. (2012) Critical review of mouse models of venous thrombosis. Arterioscler Thromb Vasc Biol. 32, 556-62. doi: 10.1161/ATVBAHA.111.244608.

Ding, Y., & Bromberg, J.S. (2012) Regulatory T cell migration during an immune response. Trends Immunol. 33, 174-80. doi: 10.1016/j.it.2012.01.002.

Dinh, T.N., Kyaw, T.S., Kanellakis, P., To, K., Tipping, P., Toh, B.H., Bobik, A., & Agrotis, A. (2012) Cytokine therapy with interleukin-2/anti-interleukin-2 monoclonal antibody complexes expands CD4+CD25+Foxp3+ regulatory T cells and attenuates development and progression of atherosclerosis. Circulation.126, 1256-66. doi: 10.1161/ CIRCULATIONAHA.112. 099044.

Domínguez, P.M., & Ardavín, C. (2010) Differentiation and function of mouse monocyte-derived dendritic cells in steady state and inflammation. Immunol Rev. 234, 90-104. doi: 10.1111/j.0105-2896.2009.00876.x.

Engelmann, B., & Massberg, S. (2013) Thrombosis as an intravascular effector of innate immunity. Nat Rev Immunol. 13, 34-45. doi: 10.1038/nri3345.

Esmon, C.T. (2008) Crosstalk between inflammation and thrombosis. Maturitas. 61,122-31. doi: 10.1016/j.maturitas.2003.10.01.

Esmon, C.T. (2009) Basic mechanisms and pathogenesis of venous thrombosis. Blood Rev. 23, 225-9. doi: 10.1016/j.blre.2009.07.002.

Evans, C.E., Grover, S.P., Humphries, J., Saha, P., Patel, AP., Patel, A.S., Lyons, O.T., Waltham, M., Modarai, B., & Smith, A. (2014) Antiangiogenic therapy inhibits venous thrombus resolution. Arterioscler Thromb Vasc Biol. 34, 565-70. doi: 10.1161/ATVBAHA. 113.302998.

Fahlén, L., Read, S., Gorelik, L., Hurst, S.D., Coffman, R.L., Flavell, R.A., & Powrie, F. (2005) T cells that cannot respond to TGF-beta escape control by CD4 (+) CD25(+) regulatory T cells. J Exp Med. 201, 737-46. doi: 10.1084/jem.20040685.

Feng, Y., van der Veeken, J., Shugay, M., Putintseva, E.V., Osmanbeyoglu, H.U., Dikiy, S., Hoyos, B.E., Moltedo, B., Hemmers, S., Treuting, P., Leslie, C.S., Chudakov, D.M., & Rudensky, A.Y. (2015) A mechanism for expansion of regulatory T-cell repertoire and its role in self-tolerance. Nature. 528, 132-6. doi: 10.1038/nature16141.

Feuerer, M., Herrero, L., Cipolletta, D., Naaz, A., Wong, J., Nayer, A., & Mathis, D. (2009) Lean, but not obese, fat is enriched for a unique population of regulatory T cells that affect metabolic parameters. Nat Med. 15, 930-9. doi: 10.1038/nm.2002.

Foks, A.C., Lichtman, A.H., & Kuiper, J. (2015) Treating atherosclerosis with regulatory T cells. Arterioscler Thromb Vasc Biol. 35, 280-7. doi: 10.1161/ATVBAHA.114.303568.

Fontenot, J.D., Gavin, M.A., & Rudensky, A.Y. (2003) Foxp3 programs the development and function of CD4+CD25+ regulatory T cells. Nat Immunol. 4, 330-6. doi :10.1038/ni904.

Fu, H., Kishore, M., Gittens, B., Wang, G., Coe, D., Komarowska, I., Infante, E., Ridley, A.J., Cooper, D., Perretti, M., & Marelli-Berg, F.M. (2014) Self-recognition of the endothelium enables regulatory T-cell trafficking and defines the kinetics of immune regulation. Nat Commun. 5, 34-6. doi: 10.1038/ncomms4436.

Furie, B., & Furie, B.C. (2008) Mechanisms of thrombus formation. N Engl J Med. 359, 938-49. doi: 10.1056/NEJMra0801082.

Geddings, J., Aleman, M.M., Wolberg, A., von Brühl, M.L., Massberg, S., & Mackman, N. (2014) Strengths and weaknesses of a new mouse model of thrombosis induced by inferior vena cava stenosis: communication from the SSC of the ISTH. J Thromb Haemost. 12, 571-3. doi: 10.1111/jth.12510.

Geuking, M.B., Cahenzli, J., Lawson, M.A., Ng, D.C., Slack, E., Hapfelmeier, S., McCoy, KD., & Macpherson, A.J. (2011) Intestinal bacterial colonization induces mutualistic regulatory T cell responses. Immunity. 34, 794-806. doi: 10.1016/j.immuni.2011.03.021.

Glatigny, S., Duhen, R., Arbelaez, C., Kumari, S., & Bettelli, E. (2015) Integrin alpha L controls the homing of regulatory T cells during CNS autoimmunity in the absence of integrin alpha 4. Sci Rep. 5, 7834. doi: 10.1038/srep07834.

Gosselin, D., Link, V.M., Romanoski, C.E., Fonseca, G.J., Eichenfield, D.Z., Spann, N.J., Stender, J.D., Chun, H.B., Garner, H., Geissmann, F., Glass, C.K. (2014) Environment drives selection and function of enhancers controlling tissue-specific macrophage identities. Cell. 159, 1327-40. doi: 10.1016/j.cell.2014.11.023.

Gottschalk, R.A., Corse, E., & Allison, J.P. (2012) Expression of Helios in peripherally induced Foxp3+ regulatory T cells. J Immunol. 188, 976-80. doi: 10.4049/jimmunol.1102964.

Gratz, I.K., & Campbell, D.J. (2014) Organ-specific and memory Treg cells: specificity, development, function, and maintenance. Front Immunol. 15, 333. doi: 10.3389/fimmu. 2014.00333.

Gu, Y., Bai, Y., Wu, J., Hu, L., & Gao, B. (2010) Establishment and characterization of an experimental model of coronary thrombotic microembolism in rats. Am J Pathol. 177, 1122-30. doi: 10.2353/ajpath.2010.090889.

Heit, JA., & Whit,e R.H. (2016) The epidemiology of venous thromboembolism. J Thromb Thrombolysis. 41, 3-14. doi: 10.1007/s11239-015-1311-6.

Hendrix, A.Y., & Kheradmand, F. (2017) The role of matrix metalloproteinases in development, repair, and destruction of the lungs. Prog Mol Biol Transl Sci. 148, 1-29. doi :10.1016/ bs.pmbts.2017.04.004.

Henke, P.K. (2007) Plasmin and matrix metalloproteinase system in deep venous thrombosis resolution. Vascular. 15, 366-71. doi: 10.2310/6670.2007.00050.

Henke, P.K., & Comerota, A.J. (2011) An update on etiology, prevention, and therapy of postthrombotic syndrome. J Vasc Surg. 53, 500-9. doi: 10.1016/j.jvs.2010.08.050.

Henke, P.K., & Wakefield, T. (2009) Thrombus resolution and vein wall injury: dependence on chemokines and leukocytes. Thromb Res. 123, S72-8. doi: 10.1016/ S00493848(09) 70148-3.

Hinz, B., Celetta, G., Tomasek, J.J., Gabbiani, G., & Chaponnier, C. (2001) Alpha-smooth muscle actin expression upregulates fibroblast contractile activity. Mol Biol Cell. 12, 2730-41. doi: 10.1091/mbc.12.9.2730.

Hinz, B., Celetta, G., Tomasek, J.J., Gabbiani, G., & Chaponnier, C. (2001) Alpha-smooth muscle actin expression upregulates fibroblast contractile activity. Mol Biol Cell. 12, 2730-41. doi: 10.1091/mbc.12.9.2730.

Hirota, K., Yoshitomi, H., Hashimoto, M., Maeda, S., Teradaira, S., Sugimoto, N., Yamaguchi, T., Nomura, T., Ito, H., Nakamura, T., Sakaguchi, N., & Sakaguchi, S. (2007) Preferential recruitment of CCR6-expressing Th17 cells to inflamed joints via CCL20 in rheumatoid arthritis and its animal model. J Exp Med. 204, 2803-12. doi: 10.1084/jem. 20071397.

Horwitz, D.A., Zheng, S.G., Wang, J., & Gray, J.D. (2008) Critical role of IL-2 and TGF-beta in generation, function and stabilisation of Foxp3+CD4+ Treg. Eur J Immunol. 38, 912-5. doi: 10.1002/eji.200738109.

Huang, M.T., Lin, B.R., Liu, W.L., Lu, C.W., & Chiang, B.L. (2016) Lymph node trafficking of regulatory T cells is prerequisite for immune suppression. J Leukoc Biol. 99, 561-8. doi: 10.1189/jlb.1A0715-296R.

Huehn, J., Siegmund, K., Lehmann, J.C., Siewert, C., Haubold, U., Feuerer, M., Debes, G.F., Lauber, J., Frey, O., Przybylski, G.K., Niesner, U., de la Rosa, M., Schmidt, C.A., Bräuer, R., Buer, J., Scheffold, A., & Hamann, A. (2004) Developmental stage, phenotype, and migration distinguish naive- and effector/memory-like CD4+ regulatory T cells. J Exp Med. 199, 303-13. doi: 10.1084/jem.20031562.

Jordan, M.S., Boesteanu, A., Reed, A.J., Petrone, A.L., Holenbeck, A.E., Lerman, M.A., Naji, A., & Caton, A.J. (2001) Thymic selection of CD4+CD25+ regulatory T cells induced by an agonist self-peptide. Nat Immunol. 2, 301-6. doi: 10.1038/86302.

Josefowicz, S.Z., & Rudensky, AY. (2009) Control of regulatory T cell lineage commitment and maintenance. Immunity. 30, 616-25. doi: 10.1016/j.immuni.2009.04.009.

Josefowicz, S.Z., Lu, L.F., & Rudensky, A.Y. (2012) Regulatory T cells: mechanisms of differentiation and function. Annu Rev Immunol. 30, 531-64. doi: 10.1146/annurev.immunol.25.022106. 141623.

Kaplan, A., Altara, R., Eid, A., Booz, G.W., & Zouein FA. (2016) Update on the Protective Role of Regulatory T Cells in Myocardial Infarction: A Promising Therapy to Repair the Heart. J Cardiovasc Pharmacol. 68, 401-13. doi: 10.1097/FJC.0000000000000436.

Kellermair, J., Redwan, B., Alias, S., Jabkowski, J., Panzenboeck, A., Kellermair, L., Winter, M.P., Weltermann, A., & Lang, I.M. (2013) Platelet endothelial cell adhesion molecule 1 deficiency misguides venous thrombus resolution. Blood. 122, 3376-84. doi: 10.1182/blood-2013-04-499558.

Kim, H.J., Barnitz, R.A., Kreslavsky, T., Brown, F.D., Moffett, H., Lemieux, M.E., Kaygusuz, Y., Meissner, T., Holderried, T.A., Chan, S., Kastner, P., Haining, W.N., & Cantor, H. (2015) Stable inhibitory activity of regulatory T cells requires the transcription factor Helios. Science. 350, 334-9. doi: 10.1126/science.aad0616.

Kohlmeier, J.E., Cookenham, T., Roberts, A.D., Miller, S.C., & Woodland, D.L. (2010) Type I interferons regulate cytolytic activity of memory CD8(+) T cells in the lung airways during respiratory virus challenge. Immunity. 33, 96-105. doi: 10.1016/j.immuni. 2010.06.016.

Kurtulus, S., Sakuishi, K., Ngiow, S.F., Joller, N., Tan, D.J., Teng, M.W., Smyth, M.J., Kuchroo, V.K., & Anderson, A.C. (2015) TIGIT predominantly regulates the immune response via regulatory T cells. J Clin Invest. 125, 4053-62. doi: 10.1172/JCI81187.

Lahl, K., & Sparwasser T. (2011) In vivo depletion of FoxP3+ Tregs using the DEREG mouse model. Methods Mol Biol. 707, 157-72. doi: 10.1007/978-1-61737-979-6-10.

Lahl, K., Loddenkemper, C., Drouin, C., Freyer, J., Arnason, J., Eberl, G., Hamann, A., Wagner, H., Huehn, J., & Sparwasser, T. (2007) Selective depletion of Foxp3+ regulatory T cells induces a scurfy-like disease. J Exp Med. 204, 57-63. doi: 10.1084/jem.20061852.

Laurance, S., Bertin, F.R., Ebrahimian, T., Kassim, Y., Rys, R.N., Lehoux, S., Lemarié, C.A., & Blostein, M.D. (2017) Gas6 promotes inflammatory (CCR2hiCX3CR1lo) monocyte recruitment in venous thrombosis. Arterioscler Thromb Vasc Biol. 37, 1315-22. doi:10.1161/ATVBAHA. 116.308925.

Lavin, Y., Winter, D., Blecher-Gonen, R., David, E., Keren-Shaul, H., Merad, M., Jung, S., & Amit, I. (2014) Tissue-resident macrophage enhancer landscapes are shaped by the local microenvironment. Cell. 159, 1312-26. doi: 10.1016/j.cell.2014.11.018.

Lertkiatmongkol, P., Liao, D., Mei, H., Hu, Y., & Newman, P.J. (2016) Endothelial functions of platelet/endothelial cell adhesion molecule-1 (CD31). Curr Opin Hematol. 23, 253-9. doi: 10.1097/MOH.0000000000000239.

Létourneau, S., van Leeuwen, E.M., Krieg, C., Martin, C., Pantaleo, G., Sprent, J., Surh, C.D., & Boyman, O. (2010) IL-2/anti-IL-2 antibody complexes show strong biological activity by avoiding interaction with IL-2 receptor alpha subunit CD25. Proc Natl Acad Sci. 107, 2171-6. doi: 10.1073/pnas.0909384107.

Levine, A.G., Arvey, A., Jin, W., & Rudensky, A.Y. (2014) Continuous requirement for the TCR in regulatory T cell function. Nat Immunol. 15, 1070-8. doi: 10.1038/ni.3004.

Ley, K., Miller, Y.I., & Hedrick, C.C. (2011) Monocyte and macrophage dynamics during atherogenesis. Arterioscler Thromb Vasc Biol. 31, 1506-16. doi: 10.1161/ATVBAHA. 110.221127.

Li-Fan, L.u., & Rudensky, AY. (2009) Molecular orchestration of differentiation and function of regulatory T cells. Genes Dev. 23, 1270-82. doi: 10.1101/gad.1791009.

Li, X., & Zheng, Y. (2015) Regulatory T cell identity: formation and maintenance. Trends Immunol. 36, 344-53. doi: 10.1016/j.it.2015.04.006.

Liston, A., & Gray, D.H. (2014) Homeostatic control of regulatory T cell diversity. Nat Rev Immunol. 14, 154-65. doi: 10.1038/nri3605.

Liu Cassado, A. (2017) F4/80 as a major macrophage marker: the case of the peritoneum and spleen. Results Probl Cell Differ. 62, 161-79. doi: 10.1007/978-3-319-54090-0.

Liu, L., & Shi, G.P. (2012) CD31: beyond a marker for endothelial cells. Cardiovasc Res. 94, 3-5. doi: 10.1093/cvr/cvs108.

Luther, N., Shahneh, F., Brähler, M., Krebs, F., Jäckel, S., Subramaniam, S., Stanger, C., Schönfelder, T., Kleis-Fischer, B., Reinhardt, C., Probst, H.C., Wenzel, P., Schäfer, K., & Becker, C. (2016) Innate Effector-Memory T-Cell Activation Regulates Post-Thrombotic Vein Wall Inflammation and Thrombus Resolution. Circ Res. 119, 1286-95. doi: 10.1161/CIRCRESAHA.116.309301.

Mackman N. (2008) Triggers, targets and treatments for thrombosis. Nature. 451, 914-8. doi: 10.1038/nature06797.

Mackman, N. (2012) New insights into the mechanisms of venous thrombosis. J Clin Invest.122, 2331-6. doi: 10.1172/JCI60229.

Malek, T.R., & Castro, I. (2010) Interleukin-2 receptor signalling: at the interface between tolerance and immunity. Immunity. 33, 153-65. doi: 10.1016/j.immuni.2010.08.004.

Mayer, C.T., Lahl, K., Milanez-Almeida, P., Watts, D., Dittmer, U., Fyhrquist, N., Huehn, J., Kopf, M., Kretschmer, K., Rouse, B., & Sparwasser, T. (2014) Advantages of Foxp3 (+) regulatory T cell depletion using DEREG mice. Immun Inflamm Dis. 2, 162-5. doi: 10.1002/iid3.33.

Molofsky, A.B., Savage, A.K., & Locksley, R.M. (2015) Interleukin-33 in tissue homeostasis, injury, and inflammation. Immunity. 42, 1005-19. doi: 10.1016/j.immuni.2015.06.006.

Nahrendorf, M., Pittet, M.J., & Swirski, F.K. (2010) Monocytes: protagonists of infarct inflammation and repair after myocardial infarction. Circulation. 2010, 121, 2437-45. doi: 10.1161/ CIRCULATIONAHA. 109.916346.

Nguyen, K.P., McGilvray, K.C., Puttlitz, C.M., Mukhopadhyay, S., Chabasse, C., & Sarkar, R. (2015) Matrix metalloproteinase 9 (MMP-9) regulates vein wall biomechanics in murine thrombus resolution. PLoS One. 10, e0139145. doi: 10.1371/journal.pone. 0139145.

Nissinen, L., Kähäri, V.M. (2014) Matrix metalloproteinases in inflammation. Biochim Biophys 1840, 2571-80. doi: 10.1016/j.bbagen.2014.03.007.

Pabbisetty, S.K., Rabacal, W., Volanakis, E.J., Parekh, V.V., Olivares-Villagómez, D., Cendron, D., Boyd, K.L., Van Kaer, L., & Sebzda, E. (2016) Peripheral tolerance can be modified by altering KLF2-regulated Treg migration. Proc Natl Acad Sci. 113, E4662-70. doi: 10.1073/pnas.1605849113.

Panduro, M., Benoist, C., & Mathis, D. (2016) Tissue Tregs. Annu Rev Immunol. 34, 609-33. doi: 10.1146/annurev-ommunol-032712-095948.

Qu, C., Brinck-Jensen, N.S., Zang, M., & Chen, K. (2014) Monocyte-derived dendritic cells: targets as potent antigen-presenting cells for the design of vaccines against infectious diseases. Int J Infect Dis. 19, 1-5. doi: 10.1016/j.ijid.2013.09.023.

Rosenblum, M.D., Way, S.S., & Abbas, A.K. (2016) Regulatory T cell memory. Nat Rev Immunol. 16, 90-101. doi: 10.1038/nri.2015.1.

Roumen-Klappe, E.M., Janssen, M.C., Van Rossum, J., Holewijn, S., Van Bokhoven, M.M., Kaasjager, K., Wollersheim, H., & Den Heijer, M. (2009) Inflammation in deep vein thrombosis and the development of post-thrombotic syndrome: a prospective study. J Thromb Haemost. 7, 582-7. doi: 10.1111/j.1538-7836.2009.03286.x.

Rzucidlo, E.M., Martin, K.A., & Powell, R.J. (2007) Regulation of vascular smooth muscle cell differentiation. J Vasc Surg. 45, 25-32. doi: 10.1016/j.jvs.2007.03.001.

Safinia, N., Scotta, C., Vaikunthanathan, T., Lechler, R.I., & Lombardi, G. (2015) Regulatory T cells: serious contenders in the promise for immunological tolerance in transplantation. Front Immunol. 6, 438. doi: 10.3389/fimmu.2015.00438.

Sage, P.T., & Sharpe, A.H. (2016) T follicular regulatory cells. Immunol Rev. 271, 246-59. doi: 10.1111/imr.12411.

Saha, P., Humphries, J., Modarai, B., Mattock, K., Waltham, M., Evans, C.E., Ahmad, A., Patel, A.S., Premaratne, S., Lyons, O.T., & Smith, A. (2011) Leukocytes and the natural history of deep vein thrombosis: current concepts and future directions. Arterioscler Thromb Vasc Biol. 31(3), 506-12. doi: 10.1161/ATVBAHA.110.213405.

Sakaguchi, S., Yamaguchi, T., Nomura, T., & Ono, M. (2008) Regulatory T cells and immune tolerance. Cell. 133, 775-87. doi: 10.1016/j.cell.2008.05.009.

Schiering, C., Krausgruber, T., Chomka, A., Fröhlich, A., Adelmann, K., Wohlfert, E.A., Pott, J., Griseri, T., Bollrath, J., Hegazy, A.N., Harrison, O.J., Owens, B.M.J., Löhning, M., Belkaid, Y., Fallon, P.G., & Powrie, F. (2014) The alarmin IL-33 promotes regulatory T-cell function in the intestine. Nature. 513, 564-8. doi: 10.1038/nature13577.

Schönfelder, T., Jäckel, S., & Wenzel, P. (2017) Mouse models of deep vein thrombosis. Gefasschirurgie. 22, 28-33. doi: 10.1007/s00772-016-0227-6.

Schulz, C., Engelmann, B., & Massberg, S. (2013) Crossroads of coagulation and innate immunity: the case of deep vein thrombosis. J Thromb Haemost. 11, 233-41. doi: 10.1111/ jth.12261.

Shevach, E.M. (2009) Mechanisms of Foxp3+ T regulatory cell-mediated suppression. Immunity. 30, 636-45. doi: 10.1016/j.immuni.2009.04.010.

Shi, C., & Pamer, E.G. (2011) Monocyte recruitment during infection and inflammation. Nat Rev Immunol. 11, 762-74. doi: 10.1038/nri3070.

Shiow, L.R., Rosen, D.B., Brdicková, N., Xu, Y., An, J., Lanier, L.L., Cyster, J.G., Matloubian, M. (2006) CD69 acts downstream of interferon-alpha/beta to inhibit S1P1 and lymphocyte egress from lymphoid organs. Nature. 440, 540-4. doi: 10.1038/ nature04606.

Skon, C.N., Lee, J.Y., Anderson, K.G., Masopust, D., Hogquist, K.A., & Jameson, S.C. (2013) Transcriptional downregulation of S1pr1 is required for the establishment of resident memory CD8+ T cells. Nat Immunol. 14, 1285-93. doi: 10.1038/ni.2745.

Smigiel, K.S., Richards, E., Srivastava, S., Thomas, K.R., Dudda, J.C., Klonowski, K.D., & Campbell, D.J. (2014) CCR7 provides localized access to IL-2 and defines

homeostatically distinct regulatory T cell subsets. J Exp Med. 13, 121-36. doi: 10.1084/jem.20131142.

Sojka, D.K., Huang, Y.H., & Fowell, D.J. (2008) Mechanisms of regulatory T-cell suppression- a diverse arsenal for a moving target. Immunology. 124, 13-22. doi:10.1111/j.1365-2567.2008.02813.x.

Sprouse, M.L., Scavuzzo, M.A., Blum, S., Shevchenko, I., Lee, T., Makedonas, G., Borowiak, M., Bettini M.L., & Bettini, M. (2018) High self-reactivity drives T-bet and potentiates Treg function in tissue-specific autoimmunity. JCI Insight. 3, 97322. doi: 10.1172/jci.insight.97322.

Streiff, M.B., Agnelli, G., Connors, J.M., Crowther, M., Eichinger, S., Lopes, R., McBane, R.D., Moll, S., & Ansell, J. (2016) Guidance for the treatment of deep vein thrombosis and pulmonary embolism. J Thromb Thrombolysis. 41, 32-67. doi: 10.1007/s11239-015-1317-0.

Swystun, L.L., & Liaw, P.C. (2016) The role of leukocytes in thrombosis. Blood. 128, 753-62. doi: 10.1182/blood-2016-05-718114.

Szurek, E., Cebula, A., Wojciech, L., Pietrzak, M., Rempala, G., Kisielow, P., & Ignatowicz, L. (2015) Differences in expression level of helios and neuropilin-1 do not distinguish thymus-derived from extrathymically-induced CD4+Foxp3+ regulatory T cells. PLoS One. 10, e0141161. doi: 10.1371/journal.pone.0141161.

Takada, K., Wang, X., Hart, G.T., Odumade, O.A., Weinreich, M.A., Hogquist, K.A., & Jameson, S.C. (2011) Kruppel-like factor 2 is required for trafficking but not quiescence in postactivated T cells. J Immunol. 186, 775-83. doi: 10.4049/jimmunol.1000094.

Tan, T.G., Mathis, D., & Benoist, C. (2016) Singular role for T-BET+ CXCR3+ regulatory T cells in protection from autoimmune diabetes. Proc Natl Acad Sci. 113, 14103-8. doi: 10.1073/pnas.1616710113.

Tang, Q., & Bluestone, J.A. (2008) The Foxp3+ regulatory T cell: a jack of all trades, master of regulation. Nat Immunol. 9, 239-44. doi: 10.1038/ni1572.

Tanoue, T., Atarashi, K., & Honda, K. (2016) Development and maintenance of intestinal regulatory T cells. Nat Rev Immunol. 16, 295-309. doi: 10.1038/nri.2016.36.

Tauro, S., Nguyen, P., Li, B., & Geiger, T.L. (2013) Diversification and senescence of Foxp3+ regulatory T cells during experimental autoimmune encephalomyelitis. Eur J Immunol. 43, 1195-207. doi: 10.1002/eji.201242881.

Toomer, K.H., Yuan, X., Yang, J., Dee, M.J., Yu, A., Malek, T.R. (2016) Developmental progression and interrelationship of central and effector regulatory T cell subsets. J Immunol. 196, 3665-76. doi: 10.4049/jimmunol.1500595.

Undas, A., & Ariëns, R.A. (2011) Fibrin clot structure and function: a role in the pathophysiology of arterial and venous thromboembolic diseases. Arterioscler Thromb Vasc Biol. 31, e88-99. doi: 10.1161/ATVBAHA.111.230631.

van der Veeken, J., Gonzalez, A.J., Cho, H., Arvey, A., Hemmers, S., Leslie, C.S., & Rudensky A.Y. (2016) Memory of inflammation in regulatory T cells. 166, 977-90. doi: 10.1016/j.cell.2016.07.006.

van Santen, H.M., Benoist, C., & Mathis, D. (2004) Number of T reg cells that differentiate does not increase upon encounter of agonist ligand on thymic epithelial cells. J Exp Med. 200, 1221-30. doi: 10.1084/jem.20041022.

Villalta, S.A., Rosenthal, W., Martinez, L., Kaur, A., Sparwasser, T., Tidball, J.G., Margeta, M., Spencer, M.J., & Bluestone, J.A. (2014) Regulatory T cells suppress muscle inflammation and injury in muscular dystrophy. Sci Transl Med. 6, 1-10. doi: 10.1126/scitranslmed.3009925.

Vogel, B., Siebert, H., Hofmann, U., & Frantz, S. (2015) Determination of collagen content within picrosirius red stained paraffin-embedded tissue sections using fluorescence microscopy. MethodsX. 2, 124-34. doi: 10.1016/j.mex.2015.02.007.

Von Brühl, M.L., Stark, K., Steinhart, A., Chandraratne, S., Konrad, I., Lorenz, M., Khandoga A., Preissner, K.T., Engelmann, B., & Massberg, S. (2012) Monocytes, neutrophils, and platelets cooperate to initiate and propagate venous thrombosis in mice in vivo. J Exp Med, 209, 819-35. doi: 10.1084/jem.20112322.

Wakefield, T.W., Myers, D.D., & Henke, P.K. (2008) Mechanisms of venous thrombosis and resolution. Arterioscler Thromb Vasc Biol. 28, 387-91. doi: 10.1161/ATVBAHA.108.162289.

Webster, K.E., Walters, S., Kohler, R.E., Mrkvan, T., Boyman, O., Surh, C.D., Grey, S.T., & Sprent, J. (2015) In vivo expansion of T reg cells with IL-2-mAb complexes: induction of

resistance to EAE and long-term acceptance of islet allografts without immuno suppression. J Exp Med. 206, 751-60. doi: 10.1084/jem.20082824.

Wei, S., Kryczek, I., & Zou, W. (2006) Regulatory T-cell compartmentalisation and trafficking. Blood. 108, 426-31. doi: 10.1182/blood-2006-01-0177.

Wynn, T.A., & Vannella, K.M. (2016) Macrophages in tissue repair, regeneration, and fibrosis. 44, 450-62. doi: 10.1016/j.immuni.2016.02.015.

Zeisberg, E.M., Tarnavski, O., Zeisberg, M., Dorfman, A.L., McMullen, J.R., Gustafsson, E., Chandraker, A., Yuan, X., Pu, W.T., Roberts, A.B., Neilson, E.G., Sayegh, M.H., Izumo, S., & Kalluri, R. (2007) Endothelial-to-mesenchymal transition contributes to cardiac fibrosis. Nat Med. 13, 952-61. doi: 10.1038/nm1613.

Zhang, N., Schröppel, B., Lal, G., Jakubzick, C., Mao, X., Chen, D., Yin, N., Jessberger, R., Ochando, J.C., Ding, Y., & Bromberg, J.S. (2009) Regulatory T cells sequentially migrate from inflamed tissues to draining lymph nodes to suppress the alloimmune response. Immunity. 30, 458-69. doi: 10.1016/j.immuni.2008.12.022.

# 7. APPENDIX

## 7.1. LIST OF FIGURES

### CHAPTER 1. INTRODUCTION



### CHAPTER 2. MATERIALS AND METHODS

## 7.2. LIST OF TABLES

### CHAPTER 1. INTRODUCTION



### CHAPTER 2. MATERIALS AND METHODS

**CHAPTER 3. RESULTS**

## 7.3. LIST OF ABBREVIATIONS

| | |
|---|---|
| ACK | Ammonium Chloride Postassium |
| Aire | Auto Immune Regulator |
| APC | Antigen Presenting Cells |
| aSMA | a-Smooth Muscle Cell |
| BAC | Bacterial Artificial Chromosome |
| Bcl-6 | B cell Lymphoma |
| Blimp-1 | B lymphocyte induced maturation Protein |
| BSA | Bovine Serum Albumin |
| cAMP | cyclic Adenosine Monophosphate |
| CCL | CC Chemokine Ligand |
| CD | Cluster of Differentiation |
| Cre | Causes recombination |
| CRP | C- Reactive Protein |
| CTEPH | Chronic Thromboembolic Pulmonary Hypertension |
| CTLA-4 | Cytotoxic T Lymphocyte Associated protein |
| CXCL | CX Chemokine Ligand |
| CXCR | CX Chemokine Receptor |
| DCs | Dendritic Cells |
| DEREG | Depletion of Regulatory T Cells |
| DMRs | Differentially Methylated Regions |
| DNA | Deoxyribonucleid Acid |
| DT | Diphtheria Toxin |
| DTR | Diphtheria Toxin Receptor |

| | |
|---|---|
| DVT | Deep Vein Thrombosis |
| ECM | Extra Cellular Matrix |
| EDTA | Ethylenediaminetetraacetic Acid |
| EndMT | Endothelial-to-Mesenchymal Transformation |
| FACS | Fluorescence Activated Cell Sorting |
| FITC | Fluorescein Isothiocyanate |
| FN | Fibronectin |
| Foxp3 | Forkhead box P3 |
| GATA | Gata binding protein |
| GFP | Green Fluorescent Protein |
| GITR | Glucocorticoid Induced Tumour necrosis factor Receptor |
| GP | Glycoprotein |
| HFUS | High Frequency Ultra Sound |
| i.p. | intraperitoneal |
| i.v. | intravenously |
| ICOS | Inducible Costimulator |
| IDO | Indoleamine 2, 3-Dioxygenase |
| IL | Interleukin |
| IP3 | Inositol trisphosphate |
| IPEX | Immunodysregulation Polyendocrinopathy Enteropathy X-Linked |
| IRF | Interferon Regulatory Factor |
| IVC | Inferior Vena Cava |
| KLF | Krüppel Like Factor |
| MCP-1 | Monocyte Chemotactic Protein-1 |

| | |
|---|---|
| MHC | Major Histocompatibility Complex |
| MMPs | Matrix Metalloproteinases |
| mTECs | medullary Thymic Epithelial Cells |
| mTOR | mammalian Target of Rapamycin |
| NETs | Neutrophil Extracellular Traps |
| NF-κB | Nuclear Factor kappa-light-chain-enhancer of activated B cells |
| Nur | Nuclear receptor |
| PE | Pulmonary Embolism |
| PI3K | Phosphoinositide 3- kinase |
| PTS | Post-Thrombotic Syndrome |
| s.c. | subcutaneous |
| S1P1 | Sphingosine-1 Phosphate receptor type 1 |
| SP | Single Positive |
| STAT | Signal Transducer and Activator Transcription |
| t-PA | tissue-type Plasminogen Activator |
| TCR | T Cell Receptor |
| TF | Tissue Factor |
| TGF-β | Transforming Growth Factor beta |
| Th | T helper cell |
| TIGIT | T cell Ig and ITIM |
| Tregs | Regulatory T cells |
| TSAs | Tissue-Specific Antigens |
| TSDR | Treg Specific Demethylation Region |
| u-PA | urokinase-type Plasminogen Activator |

| | |
|---|---|
| VAT | Visceral Adipose Tissue |
| VSMC | Vascular Smooth Muscle Cell |
| VTE | Venous Thromboembolism |
| vWF | von Willebrand Factor |
| WT | Wild Type |
| γc | gamma-chain |

## ACKNOWLEDGEMENT

Completion of this doctoral dissertation was possible with the support of several people. I would like to express my sincere gratitude to all of them.